Single-Tap Precoders and Decoders for Multi-User MIMO FBMC-OQAM under Strong Channel Frequency Selectivity

François Rottenberg, *Student Member, IEEE,* Xavier Mestre, *Senior Member, IEEE,* François Horlin, *Member, IEEE,* and Jérôme Louveaux, *Member, IEEE*

arXiv:1611.02463v1 [cs.IT] 8 Nov 2016

Abstract

The design of linear precoders or decoders for multi-user (MU) multiple-input multiple-output (MIMO) filterbank multicarrier (FBMC) modulations in the case of strong channel frequency selectivity is presented. The users and the base station (BS) communicate using space division multiple access (SDMA). The low complexity proposed solution is based on a single tap per-subcarrier precoding/decoding matrix at the base station (BS) in the downlink/uplink. As opposed to classical approaches that assume flat channel frequency selectivity at the subcarrier level, the BS does not make this assumption and takes into account the distortion caused by channel frequency selectivity. The expression of the FBMC asymptotic mean squared error (MSE) in the case of strong channel selectivity derived in earlier works is developed and extended. The linear precoders and decoders are found by optimizing the MSE formula under two design criteria, namely zero forcing (ZF) or minimum mean squared error (MMSE). Finally, simulation results demonstrate the performance of the optimized design. As long as the number of BS antennas is larger than the number of users, it is shown that those extra degrees of freedom can be used to compensate for the channel frequency selectivity.

Index Terms

FBMC, frequency selective channel, MU MIMO.

I. Introduction

Orthogonal frequency division multiplexing (OFDM) is the most popular multicarrier modulation scheme nowadays. It is used for instance in systems such as WiFi, long term evolution (LTE) or digital video broadcasting (DVB). OFDM has been very attractive mainly because of its low complexity of implementation. The introduction of the cyclic prefix (CP) in OFDM allows for easy channel equalization. Extension to multiple-input multiple-output

François Rottenberg and Jérôme Louveaux are with the Université catholique de Louvain, 1348 Louvain-la-Neuve, Belgium (e-mail: francois.rottenberg@uclouvain.be;jerome.louveaux@uclouvain.be).

Xavier Mestre is with the Centre Tecnolgic de Telecomunicacions de Catalunya, 08860 Barcelona, Spain (e-mail: xavier.mestre@cttc.cat).

François Rottenberg and François Horlin are with the Université libre de Bruxelles, 1050 Brussel, Belgium (e-mail: fhorlin@ulb.ac.be).

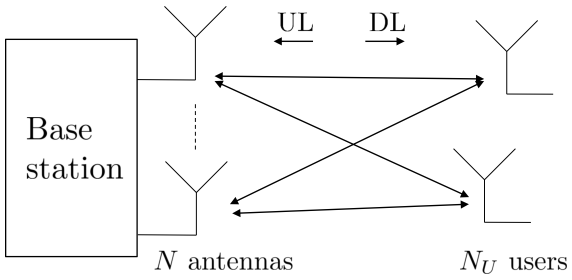

Fig. 1. Multi-user MIMO scenario: N_U single-antenna users and one base station with N antennas communicate simultaneously in UL and DL using space division multiple access.

(MIMO) scenarios is straightforward thanks to the OFDM orthogonality ensured in the complex domain. At the same time, due to the rectangular pulse shaping of the fast Fourier transform (FFT) filters, OFDM systems exhibit very high frequency leakage and poor stopband attenuation. Furthermore, the use of the CP in OFDM significantly reduces the spectral efficiency of the system.

In the light of the shortcomings of OFDM, Offset-QAM-based filterbank multicarrier (FBMC-OQAM) modulation has been regarded as an attractive alternative. Rather than using a rectangle pulse in time, FBMC-OQAM uses a pulse shape which is more spread out in time and has much larger stopband attenuation [1]. This in turn translates into higher spectral efficiency and relaxed synchronization constraints [2]. Moreover, it does not require CP overhead, which allows for a larger spectral efficiency. These advantages come at the expense of an increase in the system implementation complexity.

Under frequency selective channels, single tap equalization is sufficient in OFDM to restore the system orthogonality. The same result occurs in FBMC if the assumption of a frequency flat channel at the subcarrier level is made, which is typically verified for mildly frequency selective channels. However, as the selectivity of the channel increases, FBMC begins to suffer from inter-symbol interference (ISI) and inter-carrier interference (ICI) and the orthogonality is progressively destroyed [3], [4]. Many works in the literature have investigated this problem in the SISO case [4]–[7] and later on for the MIMO case, see [8] for recent review paper on the subject. Most of the approaches to mitigate channel frequency selectivity are based on the design of multi-tap fractionally spaced equalizers. For instance, in [9], the authors designed multi-tap decoding matrices following a frequency sampling design, i.e., they compute the time domain equalizer coefficients so that its frequency response passes through some well chosen target frequency points. On the other hand, [10] proposes a multi-tap filtering solution at both transmit and receive sides. This problem has also been analyzed in the MU MIMO context in several works. In [11], the authors extend the block diagonalization technique to FBMC systems. Through an iterative algorithm, the work of [12] alleviates the dimensionality constraint of [11] by allowing designs where the total number of receive antennas of the users exceeds the number of transmit antennas at the base station. In [13], [14], multi-tap precoders and decoders are iteratively and jointly designed. Moreover, the work originally devised for the SISO case in [3] and later extended for the MIMO case in [15], [16] proposes instead a parallel multi-stage processing architecture

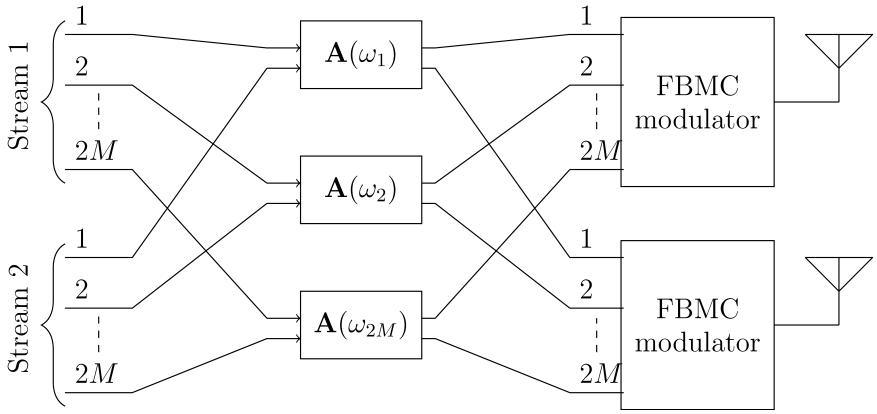

Fig. 2. Per-subcarrier precoding at the transmitter.

at both sides of the communication link. One should however note that iterative designs, multi-tap filtering and multi-stage processing increase the complexity of the system.

In this paper, in contrast to most of the proposed approaches to deal with channel frequency selectivity, we consider the classical low complexity approach based on one tap per-subcarrier precoding and decoding matrices. However, the assumption of a frequency flat channel at the subcarrier level is not made. A first order approximation of the per-subcarrier MSE for a general MIMO FBMC-OQAM system, including the effects of noise, multi-stream interference (MSI), ISI and ICI, is proposed, relying not only on the channel frequency response evaluated at this subcarrier but also on its derivatives. This approximation generalizes the one given in [16] that is valid only for the ZF case.

Furthermore, we optimize the MSE formula to design precoders and decoders in a MU MIMO context. As shown in Fig. 1, we consider a MU MIMO system with one base station (BS) and multiple single-antenna users that are not able to cooperate with each other[1]. The users and the BS are assumed to use SDMA [17, Chap. 10], i.e., they communicate simultaneously using the same time and frequency resources. Taking into account at the same time the MSI, ISI and ICI caused by channel frequency selectivity during the optimization procedure, we show that even with the very simple chosen structure, one can exploit the degrees of freedom offered by the extra BS antennas to compensate for the distortion due to frequency selectivity. In both the uplink (UL) and downlink (DL) cases, two design criteria are considered, namely zero forcing (ZF) or minimum mean squared error (MMSE). From the asymptotic study at high signal-to-noise ratio (SNR), it is shown that the first order approximation of the distortion can be completely removed as soon as the number of BS antennas is twice as large as the number of users.

The rest of this paper is structured as follows. Section II details the data model for a general FBMC-OQAM MIMO transceiver and proposes an approximation of the mean squared error (MSE) of the system under strong

[1]Note that one could straightforwardly apply the results of this paper to a point-to-point (PTP) communication link transmitting with pure spatial multiplexing.

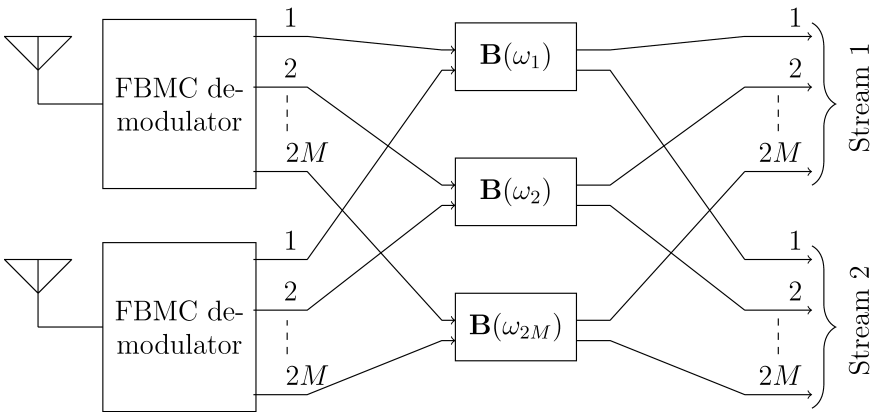

Fig. 3. Per-subcarrier decoding at the receiver.

channel frequency selectivity. Section III optimizes the previously derived MSE formula for a MU MIMO scenario as a function of the linear precoder or decoder and under a ZF or a minimum mean squared error (MMSE) criterion. Section IV validates the accuracy of MSE approximation and the performance of the linear precoder and decoder through simulations. Finally, Section V concludes the paper and appendixes contain the mathematical proof of previous sections.

A. Notations

Vectors and matrices are denoted by bold lowercase and uppercase letters, respectively. Superscripts *, ^{T} and ^{H} stand for conjugate, transpose and Hermitian operators. tr, $\mathbb{E}$, $\Im$ and $\Re$ denote the trace, expectation, imaginary and real parts respectively. Symbol $O\left(M^{-\ell}\right)$ denotes a matrix of possibly increasing dimensions whose entries decay to zero faster than $M^{-\ell}$.

II. MSE Formulation for General MIMO FBMC-OQAM System Under Strong Channel Frequency Selectivity

We will first introduce the system model for a general MIMO FBMC-OQAM transmission and then give an approximation of the MSE at the output of the transceiver chain.

A. General MIMO FBMC-OQAM transmission

Let us consider a MIMO FBMC-OQAM system with N_T and N_R antennas at the transmit and receive sides, respectively. The number of real-valued multicarrier symbols is denoted by $2N_s$ and the number of streams by S.

Multicarrier modulations divide the transmission band into multiple narrow bands. If the number of subcarriers, denoted by $2M$, is large enough with respect to (w.r.t.) the channel delay spread, a common assumption is to assume that the channel is approximately frequency flat inside each sub-band so that precoding (pre-equalization) and decoding (equalization) operations can be performed at the subcarrier level. The block diagrams of the transmitter and

receiver are depicted in Fig. 2 and Fig. 3. At the transmitter, the precoding matrix at the m-th subcarrier is denoted by $\mathbf{A}(\omega_m) \in \mathbb{C}^{N_T \times S}$. At the receiver, the decoding matrix at the m-th subcarrier is denoted by $\mathbf{B}(\omega_m) \in \mathbb{C}^{S \times N_R}$.

The real-valued transmitted symbols denoted by $\mathbf{d}_{l,m} \in \mathbb{R}^{S \times 1}$ are first precoded and then FBMC-OQAM modulated using a prototype pulse $p[n]$ of length L_p. The transmitted signal at the different transmit antennas, denoted by $\mathbf{s}[n] \in \mathbb{C}^{N_T \times 1}$, is given by

$$\mathbf{s}[n] = \sum_{l=0}^{2N_s-1} \sum_{m=0}^{2M-1} \mathbf{A}(\omega_m)\mathbf{d}_{l,m}p_{l,m}[n]$$

where $p_{l,m}[n] = \frac{j^{l+m}}{M} p[n - lM]e^{j\frac{2\pi}{2M}m(n-\frac{L_p-1}{2})}$. We denote by $\mathbf{H}(\omega) \in \mathbb{C}^{N_R \times N_T}$ the channel frequency response matrix. The signal at the different receive antennas, denoted by $\mathbf{r}[n] \in \mathbb{C}^{N_R \times 1}$, is given by

$$\mathbf{r}[n] = \sum_{b=-\infty}^{+\infty} \mathcal{H}[b]\mathbf{s}[n-b] + \mathbf{w}[n]$$

where $\mathcal{H}[b] = \frac{1}{2\pi}\int_0^{2\pi} \mathbf{H}(\omega)e^{j\omega b}d\omega$ is the channel impulse response which is assumed not to change over the frame time duration. The column vector $\mathbf{w}[n]$ contains the additive white Gaussian noise samples. The received signal is FBMC-OQAM demodulated using prototype pulse $q[n]$ of length L_q. The signal after demodulation and decoding (equalization), at subcarrier l_0 and multicarrier symbol m_0, denoted by $\mathbf{x}_{l_0,m_0} \in \mathbb{C}^{S \times 1}$, may be written as

$$\mathbf{x}_{l_0,m_0} = \mathbf{B}(\omega_{m_0}) \sum_{n=0}^{L_q-1} \mathbf{r}[n]q^*_{l_0,m_0}[n]$$

where $q_{l_0,m_0}[n] = \frac{j^{l_0+m_0}}{M}\tilde{q}[n-l_0M]e^{j\frac{2\pi}{2M}m_0(n-\frac{L_q-1}{2})}$ and where $\tilde{q}[n]$ is the reversed version of the receive prototype, namely $\tilde{q}[n] = q[L_q - 1 - n]$. Finally the estimated symbols are obtained by taking the real part, i.e., $\hat{\mathbf{d}}_{l_0,m_0} = \Re\{\mathbf{x}_{l_0,m_0}\}$.

B. MSE formulation

We define the MSE at the output of the transceiver chain corresponding to all streams as[2]

$$\begin{aligned}\mathrm{MSE}(m) &= 2\mathbb{E}\left(\|\hat{\mathbf{d}}_{l,m} - \mathbf{d}_{l,m}\|^2\right) \\ &= P_d(m) + N_0\mathrm{tr}\left[\mathbf{B}(\omega_m)\mathbf{B}(\omega_m)^H\right] \end{aligned} \quad (1)$$

where N_0 is the noise power and the expectation is taken over transmitted symbols and noise. Since noise and symbols are uncorrelated, their effect can be separated in the two terms of (1). The term $P_d(m)$ corresponds to the distortion due to MSI, ISI and ICI. The designs of Fig. 2 and Fig. 3 usually rely on channel frequency flatness at the subcarrier level. When the variation of the channel becomes non-negligible, this assumption becomes inaccurate and distortion will increase with the appearance of MSI, ISI and ICI (, i.e., the term $P_d(m)$ increases). To be able to give an analytical expression of $P_d(m)$, we make the following assumptions:

$(\mathbf{As1})$ The actual precoding and decoding matrices implemented at the m-th subcarrier result from the evaluation of the functions $\mathbf{A}(\omega)$ and $\mathbf{B}(\omega)$ at frequency $\omega_m = \frac{2\pi(m-1)}{2M}$. The precoder, decoder and channel frequency

[2]Observe that we introduce the factor 2 in order to consider the distortion of the complex symbols, and not the real ones.

response matrices, $\mathbf{A}(\omega) \in \mathbb{C}^{N_T \times S}$, $\mathbf{B}(\omega) \in \mathbb{C}^{S \times N_R}$ and $\mathbf{H}(\omega) \in \mathbb{C}^{N_R \times N_T}$, are twice differentiable functions of the frequency ω on the torus $\mathbb{R}/2\pi\mathbb{Z}$.

$(\mathbf{As2})$ The prototype pulse $p[n]$ is assumed identical at transmit and receive sides, so that $p[n] = q[n]$. It is either symmetric or anti-symmetric in the time domain and it meets the perfect reconstruction (PR) conditions. It has length $2M\kappa$, where κ is the overlapping factor. Furthermore, $p[n]$ is obtained by discretization of a smooth real-valued analog waveform $p(t)$, which is a $\mathcal{C}^\infty\left([-T_s\kappa/2, T_s\kappa/2]\right)$ function, so that

$$p[n] = p\left(\left(n - \frac{2M\kappa+1}{2}\right)\frac{T_s}{2M}\right),\ n = 1, \ldots, 2M\kappa$$

where T_s is the multicarrier symbol period. Furthermore, the pulse $p(t)$ and its derivatives are null at the end-points of the support, namely at $t = \pm T_s\kappa/2$.

Thanks to the above assumption, we can define $p^{(r)}[n]$ as the sampled version of the r-th derivative of $p(t)$, that is

$$p^{(r)}[n] = T_s^r p^{(r)}\left(\left(n - \frac{2M\kappa+1}{2}\right)\frac{T_s}{2M}\right), n = 1, \ldots, 2M\kappa.$$

$(\mathbf{As3})$ The real-valued symbols $\mathbf{d}_{l,m}$ are independent, identically distributed bounded random variables with zero mean and variance $P_s/2$.

We are now in a position to introduce the main result of this section.

Theorem II.1. *Under* $(\mathbf{As1}) - (\mathbf{As3})$*, the MSE of the complex symbols at the* m*-th subcarrier can be expressed as*

$$\begin{aligned}
P_d(m) = {} & P_s tr\left[\left(\mathbf{BHA} - \mathbf{I}\right)\left(\mathbf{BHA} - \mathbf{I}\right)^H\right] \\
& + \frac{2\eta_{1010}^{(+,-)}}{(2M)^2} tr\left[\left(\mathbf{BH'A}\right)\left(\mathbf{BH'A}\right)^H\right] \\
& + \frac{2\eta_{1010}^{(+,-)}}{(2M)^2} \Re tr\left[\left(\mathbf{BHA} - \mathbf{I}\right)\left(\mathbf{BH''A}\right)^H\right] \\
& + \frac{4\left(\eta_{1010}^{(+,-)} + \eta_{0011}^{(-,+)}\right)}{(2M)^2} tr\left[\Im\left(\mathbf{BHA} - \mathbf{I}\right)\Im^T\left(\mathbf{B}\left(\mathbf{HA'}\right)'\right)\right] \\
& + \frac{4\left(\eta_{1010}^{(+,-)} + \eta_{0011}^{(-,+)}\right)}{(2M)^2} tr\left[\Im\left(\mathbf{BHA'}\right)\Im^T\left(\mathbf{B}\left(\mathbf{HA}\right)'\right)\right] \\
& + O\left(M^{-2}\right),
\end{aligned} \tag{2}$$

where $\eta_{1010}^{(+,-)}$ *and* $\eta_{0011}^{(-,+)}$ *are pulse-related quantities defined in Appendix A,* $'$ *and* $''$ *refer to the first and second derivatives and where all frequency-depending matrices are evaluated at* $\omega = \omega_m$*, e.g.* $\mathbf{A} = \mathbf{A}(\omega_m)$*,* $\mathbf{H}' = \mathbf{H}'(\omega_m)$*...*

Proof: See Appendix A. ■

Comments: equations (1) and (2) show that the MSE expression is composed of many terms including the effects of noise, MSI, ISI and ICI. One may recognize some usual terms, i.e., the noise term in (1) or the first term of

TABLE I

SUMMARY OF THE DIFFERENT DESIGNS UNDER CONSIDERATION AND THEIR RESPECTIVE ASSUMPTIONS.

	Decoder (Uplink, MAC channel) $\mathbf{A}_{\mathrm{UL}} = \xi_{\mathrm{UL}}\mathbf{I}_{N_U}$, $\mathbf{H}_{\mathrm{UL}} \in \mathbb{C}^{N \times N_U}$	Precoder (Downlink, BC channel) $\mathbf{B}_{\mathrm{DL}} = \xi_{\mathrm{DL}}\mathbf{I}_{N_U}, \mathbf{H}_{\mathrm{DL}} \in \mathbb{C}^{N_U \times N}$
ZF ($\mathbf{BHA} = \mathbf{I}_{N_U}$)	$\xi_{\mathrm{UL}}^{\mathrm{ZF}}$ independent of ω	$\xi_{\mathrm{DL}}^{\mathrm{ZF}}$ depends on ω
MMSE ($\mathbf{BHA} \neq \mathbf{I}_{N_U}$)	$\xi_{\mathrm{UL}}^{\mathrm{MMSE}}$ independent of ω	$\xi_{\mathrm{DL}}^{\mathrm{MMSE}}$ depends on ω

(2) related to the fact that the channel is not perfectly inverted ($\mathbf{BHA} \neq \mathbf{I}_S$). Those two terms would be the only ones remaining if the channel was frequency flat ($\mathbf{H}' = \mathbf{0}$) and the precoder non-frequency selective ($\mathbf{A}' = \mathbf{0}$). Those are also the two only terms of distortion in an OFDM system if the cyclic prefix is longer than the channel length and the system well synchronized. Furthermore, the dependence of (2) on $\mathbf{H}'$ and $\mathbf{H}''$ comes directly from the fact that the channel variation breaks the FBMC-OQAM orthogonality while the dependence in the derivatives of the precoder $\mathbf{A}'$ and $\mathbf{A}''$ shows that the precoding operations on adjacent subcarriers may influence the MSE at the current subcarrier. Notice that this effect, also known as intrinsic interference, also occurs if the channel is non-varying ($\mathbf{H}' = \mathbf{0}$) but the precoder varies over the subcarriers ($\mathbf{A}' \neq \mathbf{0}$).

III. LINEAR PRECODER AND DECODER DESIGN FOR A MU MIMO SYSTEM

The goal of this section is to optimize the general MSE formulation of (1), applied to a MU MIMO scenario, as a function of the linear precoding or decoding matrices. As shown in Fig. 1, we consider a MU MIMO system with one base station (BS) equipped with N antennas and N_U users, each one equipped with a single antenna and not able to cooperate with each other[3]. The users and the BS are assumed to use SDMA, i.e., they communicate simultaneously using the same time and frequency resources. The number of streams is equal to $S = N_U$ with $N \geq N_U$. The channel frequency response matrix $\mathbf{H}(\omega)$ is assumed to be perfectly known by the BS. For the sake of clarity, $\mathbf{H}(\omega)$ is denoted by $\mathbf{H}_{\mathrm{DL}}(\omega) \in \mathbb{C}^{N_U \times N}$ when referred to the specific DL scenario and $\mathbf{H}_{\mathrm{UL}}(\omega) \in \mathbb{C}^{N \times N_U}$ resp. in the UL case.

While optimizing the decoder in UL (resp. precoder in DL), the precoder (resp. decoder) at the other end is fixed to a real positive power normalization scalar $\xi(\omega)$ since the users cannot collaborate. In the following, a per-subcarrier total transmit power P_T constraint is considered.

$$\mathrm{tr}\left[\mathbf{A}\mathbf{A}^H\right] = P_T. \tag{3}$$

Two design criteria will be investigated, namely the ZF criterion and the MMSE criterion. A summary of the different designs under study with their corresponding assumptions is given in Table I. Note that in UL, the users

[3]Note that the approach could be generalized to the case where each user terminal is equipped with multiple antennas, although the extension does not seem trivial.

cannot not precode the streams, so that $\xi_{\mathrm{UL}}(\omega)$ is frequency non-selective. Conversely, in the DL, the BS pre-equalizes the channel at the subcarrier level. This processing depends on the channel frequency response at this subcarrier and hence, the normalization factor $\xi_{\mathrm{DL}}(\omega)$ will generally depend on frequency. Finally, the computation complexity of the proposed designs will be studied.

A. Zero Forcing Design

For this design, a channel inverting constraint is considered, namely

$$\mathbf{BHA} = \mathbf{I}_{N_U}. \tag{4}$$

The channel matrix $\mathbf{H}$ is assumed full rank, which is a quite natural assumption in the considered MU MIMO scenario. Using (4) and the fact that $(\mathbf{BHA})' = \mathbf{B}(\mathbf{HA})' + \mathbf{B}'\mathbf{HA} = \mathbf{0}$, many terms of the distortion expression of (2) vanish and the MSE in (1) simplifies to

$$\begin{aligned}\mathrm{MSE}(m) = \alpha \mathrm{tr}&\left[\left(\mathbf{BH}'\mathbf{A}\right)\left(\mathbf{BH}'\mathbf{A}\right)^H\right] \\ &- (2\alpha + 2\beta)\mathrm{tr}\left[\Im(\mathbf{BHA}')\Im(\mathbf{B}'\mathbf{HA})^T\right] \\ &+ N_0 \mathrm{tr}\left[\mathbf{BB}^H\right] + O\left(2M^{-2}\right).\end{aligned} \tag{5}$$

where $\alpha = \frac{2\eta_{1010}^{(+,-)}}{(2M)^2}$, $\beta = \frac{2\eta_{0011}^{(-,+)}}{(2M)^2}$.

1) Linear Decoder (Multiple Access Channel (MAC), Uplink): In the UL case, $\mathbf{H}_{\mathrm{UL}}$ and $\mathbf{H}'_{\mathrm{UL}} \in \mathbb{C}^{N \times N_U}$ correspond to the tall channel frequency response matrix and its derivative evaluated at the subcarrier of interest. From the power normalization (3) and channel inversion (4) constraints, the general solution of the problem can be written in the following form

$$\begin{aligned}\mathbf{A}_{\mathrm{UL}}^{\mathrm{ZF}} &= \xi_{\mathrm{UL}}^{\mathrm{ZF}} \mathbf{I}_{N_U} \\ \mathbf{B}_{\mathrm{UL}}^{\mathrm{ZF}} &= \frac{1}{\xi_{\mathrm{UL}}^{\mathrm{ZF}}}\left(\mathbf{H}^{\dagger} + \tilde{\mathbf{B}}\mathbf{P}_{\mathrm{UL}}\right)\end{aligned}$$

where $\mathbf{H}_{\mathrm{UL}}^{\dagger} = (\mathbf{H}_{\mathrm{UL}}^H\mathbf{H}_{\mathrm{UL}})^{-1}\mathbf{H}_{\mathrm{UL}}^H$, $\mathbf{P}_{\mathrm{UL}} = \mathbf{I}_N - \mathbf{H}_{\mathrm{UL}}\mathbf{H}_{\mathrm{UL}}^{\dagger}$, $\xi_{\mathrm{UL}}^{\mathrm{ZF}} = \sqrt{P_T/N_U}$ and where $\tilde{\mathbf{B}}$ is a $N_U \times N$ matrix to be optimized. This shows that the decoder can be written as the left pseudo-inverse of the channel plus a matrix lying on the left null space of $\mathbf{H}_{\mathrm{UL}}$. In the trivial case $N = N_U$, the decoder is the inverse of the channel since there are no extra degrees of freedom. One can check that the second term of the distortion in (5) is null due to the fact that $\Im(\mathbf{B}_{\mathrm{UL}}^{\mathrm{ZF}}\mathbf{H}_{\mathrm{UL}}(\mathbf{A}_{\mathrm{UL}}^{\mathrm{ZF}})') = \Im\left((\xi_{\mathrm{UL}}^{\mathrm{ZF}})'/\xi_{\mathrm{UL}}^{\mathrm{ZF}}\right)\mathbf{I}_{N_U} = \mathbf{0}$ with $\xi_{\mathrm{UL}}^{\mathrm{ZF}}$ purely real and frequency non-selective. Therefore, the optimization problem can be turned into the minimization of a quadratic expression in $\tilde{\mathbf{B}}$

$$\min_{\tilde{\mathbf{B}}} \alpha\ \mathrm{tr}\left[\left(\mathbf{H}_{\mathrm{UL}}^{\dagger}\mathbf{H}'_{\mathrm{UL}} + \tilde{\mathbf{B}}\mathbf{P}_{\mathrm{UL}}\mathbf{H}'_{\mathrm{UL}}\right)\left(\mathbf{H}_{\mathrm{UL}}^{\dagger}\mathbf{H}'_{\mathrm{UL}} + \tilde{\mathbf{B}}\mathbf{P}_{\mathrm{UL}}\mathbf{H}'_{\mathrm{UL}}\right)^H\right] + \frac{N_0 N_U}{P_T}\mathrm{tr}\left[\left(\mathbf{H}_{\mathrm{UL}}^H\mathbf{H}_{\mathrm{UL}}\right)^{-1} + \tilde{\mathbf{B}}\mathbf{P}_{\mathrm{UL}}\tilde{\mathbf{B}}^H\right]. \tag{6}$$

Setting the derivative of this expression with respect to $\tilde{\mathbf{B}}^*$ to $\mathbf{0}$, we find that the optimum solution is such that

$$\tilde{\mathbf{B}} = -\mathbf{H}_{\mathrm{UL}}^{\dagger}\mathbf{H}'_{\mathrm{UL}}\left(\mathbf{H}'^H_{\mathrm{UL}}\mathbf{P}_{\mathrm{UL}}\mathbf{H}'_{\mathrm{UL}} + \frac{N_0 N_U}{P_T \alpha}\mathbf{I}_{N_U}\right)^{-1}\mathbf{H}'^H_{\mathrm{UL}} \tag{7}$$

where we used the matrix inversion lemma.

2) Linear Precoder (Broadcast Channel (BC), Downlink): In the DL case, $\mathbf{H}_{\mathrm{DL}}, \mathbf{H}'_{\mathrm{DL}} \in \mathbb{C}^{N_U \times N}$ denote the fat channel frequency response matrix and its derivative evaluated at the subcarrier of interest. From the constraints (3) and (4), the general solution can be written as

$$\mathbf{A}_{\mathrm{DL}}^{\mathrm{ZF}} = \frac{1}{\xi_{\mathrm{DL}}^{\mathrm{ZF}}} \left(\mathbf{H}_{\mathrm{DL}}^{\dagger} + \mathbf{P}_{\mathrm{DL}} \tilde{\mathbf{A}} \right)$$

$$\mathbf{B}_{\mathrm{DL}}^{\mathrm{ZF}} = \xi_{\mathrm{DL}}^{\mathrm{ZF}} \mathbf{I}_{N_U}$$

where $\mathbf{H}_{\mathrm{DL}}^{\dagger} = \mathbf{H}_{\mathrm{DL}}^{H} (\mathbf{H}_{\mathrm{DL}} \mathbf{H}_{\mathrm{DL}}^{H})^{-1}$, $\mathbf{P}_{\mathrm{DL}} = \mathbf{I}_N - \mathbf{H}_{\mathrm{DL}}^{\dagger} \mathbf{H}_{\mathrm{DL}}$ and $\xi_{\mathrm{DL}}^{\mathrm{ZF}} = \sqrt{\mathrm{tr}\left((\mathbf{H}_{\mathrm{DL}} \mathbf{H}_{\mathrm{DL}}^{H})^{-1} + \tilde{\mathbf{A}}^{H} \mathbf{P}_{\mathrm{DL}} \tilde{\mathbf{A}} \right) / P_T}$. As in the decoder case, the second term of the distortion in (5) also disappears due to the fact that $\Im((\mathbf{B}_{\mathrm{DL}}^{\mathrm{ZF}})' \mathbf{H}_{\mathrm{DL}} \mathbf{A}_{\mathrm{DL}}^{\mathrm{ZF}}) = \Im((\xi_{\mathrm{DL}}^{\mathrm{ZF}})' / \xi_{\mathrm{DL}}^{\mathrm{ZF}}) \mathbf{I}_{N_U} = \mathbf{0}$ with ξ purely real. The optimization problem then simplifies to

$$\min_{\tilde{\mathbf{A}}} \alpha \ \mathrm{tr} \left[\left(\mathbf{H}'_{\mathrm{DL}} \mathbf{H}_{\mathrm{DL}}^{\dagger} + \mathbf{H}'_{\mathrm{DL}} \mathbf{P}_{\mathrm{DL}} \tilde{\mathbf{A}} \right) \left(\mathbf{H}'_{\mathrm{DL}} \mathbf{H}_{\mathrm{DL}}^{\dagger} + \mathbf{H}'_{\mathrm{DL}} \mathbf{P}_{\mathrm{DL}} \tilde{\mathbf{A}} \right)^{H} \right] + \frac{N_0 N_U}{P_T} \mathrm{tr} \left[(\mathbf{H}_{\mathrm{DL}} \mathbf{H}_{\mathrm{DL}}^{H})^{-1} + \tilde{\mathbf{A}}^{H} \mathbf{P}_{\mathrm{DL}} \tilde{\mathbf{A}} \right],$$

the solution of which is, after applying matrix inversion lemma,

$$\tilde{\mathbf{A}} = -\mathbf{H}_{\mathrm{DL}}^{'H} \left(\mathbf{H}'_{\mathrm{DL}} \mathbf{P}_{\mathrm{DL}} \mathbf{H}_{\mathrm{DL}}^{'H} + \frac{N_0 N_U}{P_T \alpha} \mathbf{I}_{N_U} \right)^{-1} \mathbf{H}'_{\mathrm{DL}} \mathbf{H}_{\mathrm{DL}}^{\dagger}.$$

One can check that the asymptotic MSE of the optimized precoder and decoder will be exactly the same if the channels are the Hermitian of one another, *i.e.* $\mathbf{H}_{\mathrm{DL}} = \mathbf{H}_{\mathrm{UL}}^{H}$.

3) Asymptotic Study at Low and High SNR: We concentrate here on the behavior of the optimized linear decoder in the UL (MAC) channel. Similar conclusions also hold for the precoder in the DL (BC) channel. We assume that the number of users N_U and the transmit power P_T remain constant while we let N_0 go to 0 or $+\infty$ (high and low SNR respectively). At low SNR ($N_0 \to +\infty$), the expression in (7) tends to zero ($\tilde{\mathbf{B}} \to \mathbf{0}$) and the optimized decoder converges to

$$\lim_{N_0 \to \infty} \mathbf{B}_{\mathrm{UL}}^{\mathrm{ZF}} = \frac{1}{\xi_{\mathrm{UL}}^{\mathrm{ZF}}} \mathbf{H}_{\mathrm{UL}}^{\dagger}.$$

As one would expect, when noise power is large, the distortion caused by channel selectivity is comparatively negligible. The best thing to do is to use the classical pseudo-inverse of the channel to combine the signals of each antenna.

At high SNR, assuming that $\mathbf{H}'_{\mathrm{UL}}$ is of full rank N_U, the decoder converges to a limit that depends on the rank of $\mathbf{P}_{\mathrm{UL}}$. Indeed, two cases must be considered depending on whether matrix $\mathbf{H}_{\mathrm{UL}}^{'H} \mathbf{P}_{\mathrm{UL}} \mathbf{H}'_{\mathrm{UL}}$ is invertible or not. One can rewrite $\mathbf{P}_{\mathrm{UL}}$ as a function of the singular value decomposition (SVD) of $\mathbf{H}_{\mathrm{UL}}$

$$\mathbf{H}_{\mathrm{UL}} = \begin{bmatrix} \mathbf{U}_1 & \mathbf{U}_2 \end{bmatrix} \begin{bmatrix} \mathbf{\Sigma}_{N_U \times N_U} & \mathbf{0}_{N-N_U \times N_U}^{H} \end{bmatrix}^{H} \mathbf{V}^{H}.$$

We then find $\mathbf{P}_{\mathrm{UL}} = \mathbf{U}_2 \mathbf{U}_2^{H}$ where $\mathbf{U}_2$ is the $N \times N - N_U$ matrix composed of the $N - N_U$ left singular vectors of $\mathbf{H}_{\mathrm{UL}}$ associated to its zero singular values. It is then straightforward to see that the rank of $\mathbf{P}_{\mathrm{UL}}$ is the dimension of the left null space of $\mathbf{H}_{\mathrm{UL}}$,*i.e.* $N - N_U$. First, if $N - N_U \geq N_U$, matrix $\mathbf{H}_{\mathrm{UL}}^{'H} \mathbf{P}_{\mathrm{UL}} \mathbf{H}'_{\mathrm{UL}}$ is full rank and the limit becomes

$$\lim_{N_0 \to 0} \tilde{\mathbf{B}} = -\mathbf{H}_{\mathrm{UL}}^{\dagger} \mathbf{H}'_{\mathrm{UL}} \left(\mathbf{H}_{\mathrm{UL}}^{'H} \mathbf{P}_{\mathrm{UL}} \mathbf{H}'_{\mathrm{UL}} \right)^{-1} \mathbf{H}_{\mathrm{UL}}^{'H}.$$

TABLE II

COMPLEXITY OF CALCULATING THE PROPOSED PRECODERS AND DECODERS.

	Decoder (Uplink, MAC channel)	Precoder (Downlink, BC channel)
Classical ZF	$O(2NN_U^2 + N_U^3)$	$O(3NN_U^2 + N_U^3)$
Opt. ZF	$O(4NN_U^2 + 4N^2N_U + 2N_U^3)$	$O(5NN_U^2 + 4N^2N_U + 2N_U^3)$
Classical MMSE	$O(2N^2N_U + N^3)$	$O(2N^2N_U + NN_U^2 + N^3)$
Opt. MMSE	$O(5N^2N_U + N^3)$	$O(6N^2N_U + 3NN_U^2 + 2N_U^3 + N^3)$

Replacing this expression of $\tilde{\mathbf{B}}$ into (6), it can be seen that the limit of the asymptotic MSE at high SNR will tend to zero. This means that for twice as many antennas as the number of served users, we can completely remove the first order approximation of the distortion caused by channel frequency selectivity.

As for the case $N - N_U < N_U$, using the fact that $\mathbf{P}_{\mathrm{UL}} = \mathbf{U}_2\mathbf{U}_2^H$, one can reapply the matrix inversion lemma on $\tilde{\mathbf{B}}\mathbf{P}_{\mathrm{UL}}$ in order to show that the limit becomes

$$\lim_{N_0 \to 0} \tilde{\mathbf{B}}\mathbf{P}_{\mathrm{UL}} = -\mathbf{H}_{\mathrm{UL}}^{\dagger}\mathbf{H}'_{\mathrm{UL}}\mathbf{H}'^{H}_{\mathrm{UL}}\mathbf{U}_2 \left(\mathbf{U}_2^H\mathbf{H}'_{\mathrm{UL}}\mathbf{H}'^{H}_{\mathrm{UL}}\mathbf{U}_2\right)^{-1}\mathbf{U}_2^H.$$

In this case, the noise term of the MSE will tend to zero but the first order approximation of the distortion will only be partially compensated for.

We can conclude that the optimized ZF decoder and precoder can be written in a compact expression as the pseudo-inverse of the channel plus a matrix lying on the null space of the channel. This design can compensate for the degradation due to channel frequency selectivity and even completely remove the first order approximation of the distortion for twice as many BS antennas as the number of served users.

B. Minimum Mean Squared Error Design

The previous designs rely on a ZF criterion which restricts the solution domain. In the following, we do not make this assumption and we look at the general MMSE design which will achieve an optimized performance. Indeed, for low SNR situations or highly selective subchannels, inverting the channel might strongly degrade the performance. Furthermore, the channel matrix $\mathbf{H}$ does not generally need to be full rank.

1) Linear Decoder (Multiple Access Channel, Uplink): For the decoder case, due to the power normalization constraint (3), we impose

$$\mathbf{A}_{\mathrm{UL}}^{\mathrm{MMSE}} = \xi_{\mathrm{UL}}^{\mathrm{MMSE}}\mathbf{I}_{N_U}$$
$$\mathbf{B}_{\mathrm{UL}}^{\mathrm{MMSE}} = \frac{1}{\xi_{\mathrm{UL}}^{\mathrm{MMSE}}}\hat{\mathbf{B}}$$

where $\xi_{\mathrm{UL}}^{\mathrm{MMSE}} = \sqrt{\frac{P_T}{N_U}}$ and $\hat{\mathbf{B}} = \xi_{\mathrm{UL}}^{\mathrm{MMSE}}\mathbf{B}_{\mathrm{UL}}^{\mathrm{MMSE}}$ is defined to clarify the following expressions by suppressing the dependence in $\xi_{\mathrm{UL}}^{\mathrm{MMSE}}$. Hence, the imaginary terms of the distortion in (2) again disappear due to $(\mathbf{A}_{\mathrm{UL}}^{\mathrm{MMSE}})' = \mathbf{0}$

(the precoder is frequency independent) and the optimization problem takes the following quadratic form in $\hat{\mathbf{B}}$

$$\begin{aligned}\min_{\hat{\mathbf{B}}} \mathrm{MSE}(m) = &\mathrm{tr}\left[(\hat{\mathbf{B}}\mathbf{H}_{\mathrm{UL}} - \mathbf{I})(\hat{\mathbf{B}}\mathbf{H}_{\mathrm{UL}} - \mathbf{I})^H\right] \\ &+ \alpha \mathrm{tr}\left[\left(\hat{\mathbf{B}}\mathbf{H}'_{\mathrm{UL}}\right)\left(\hat{\mathbf{B}}\mathbf{H}'_{\mathrm{UL}}\right)^H\right] \\ &+ \alpha \Re\mathrm{tr}\left[(\hat{\mathbf{B}}\mathbf{H}_{\mathrm{UL}} - \mathbf{I})(\hat{\mathbf{B}}\mathbf{H}''_{\mathrm{UL}})^H\right] \\ &+ \frac{N_0 N_U}{P_T}\mathrm{tr}\left[\hat{\mathbf{B}}\hat{\mathbf{B}}^H\right].\end{aligned}$$

Setting the derivative of this expression with respect to $\hat{\mathbf{B}}^*$ to $\mathbf{0}$ yields the MMSE decoder given by,

$$\hat{\mathbf{B}} = \left(\mathbf{H}_{\mathrm{UL}}^H + \frac{\alpha}{2}\mathbf{H}_{\mathrm{UL}}''^H\right)\left(\mathbf{H}_{\mathrm{UL}}\mathbf{H}_{\mathrm{UL}}^H + \alpha\mathbf{H}'_{\mathrm{UL}}\mathbf{H}'^H_{\mathrm{UL}} + \frac{\alpha}{2}\left(\mathbf{H}_{\mathrm{UL}}\mathbf{H}''^H_{\mathrm{UL}} + \mathbf{H}''_{\mathrm{UL}}\mathbf{H}_{\mathrm{UL}}^H\right) + \frac{N_0 N_U}{P_T}\mathbf{I}_N\right)^{-1} \tag{8}$$

2) Linear Precoder (Broadcast Channel, Downlink): In the precoder case, due to the normalization constraint, we have

$$\begin{aligned}\mathbf{A}_{\mathrm{DL}}^{\mathrm{MMSE}} &= \frac{1}{\xi_{\mathrm{DL}}^{\mathrm{MMSE}}}\hat{\mathbf{A}} \\ \mathbf{B}_{\mathrm{DL}}^{\mathrm{MMSE}} &= \xi_{\mathrm{DL}}^{\mathrm{MMSE}}\mathbf{I}_{N_U}\end{aligned}$$

with $\xi_{\mathrm{DL}}^{\mathrm{MMSE}} = \sqrt{\frac{\mathrm{tr}\left[\hat{\mathbf{A}}\hat{\mathbf{A}}^H\right]}{P_T}}$. As opposed to all of the previous designs, the imaginary terms of the distortion in (2) do not cancel out. The optimization of those two terms is difficult due to the dependence in $(\mathbf{A}_{\mathrm{DL}}^{\mathrm{MMSE}})'$. The derivative implies that the optimization of the precoder of one subcarrier depends on the neighboring subcarriers and the optimization can no longer be done locally at the subcarrier level, which increases the problem complexity and is not comparable to the other designs. Hence, we propose to impose an additional constraint which cancels the imaginary terms of (2), i.e., $\Im(\mathbf{H}_{\mathrm{DL}}\mathbf{A}_{\mathrm{DL}}^{\mathrm{MMSE}}) = \mathbf{0}$. This somehow means that we have a ZF design on the imaginary part of $\mathbf{H}_{\mathrm{DL}}\mathbf{A}_{\mathrm{DL}}^{\mathrm{MMSE}}$ and a MMSE design on its real part. We then have to minimize the following Lagrangian formulation including the constraint (via the Lagrange multiplier $\mathbf{\Psi}$)

$$\begin{aligned}\min_{\hat{\mathbf{A}}} L = &\mathrm{tr}\left[(\mathbf{H}_{\mathrm{DL}}\hat{\mathbf{A}} - \mathbf{I})(\mathbf{H}_{\mathrm{DL}}\hat{\mathbf{A}} - \mathbf{I})^H\right] \\ &+ \alpha \mathrm{tr}\left[\left(\mathbf{H}'_{\mathrm{DL}}\hat{\mathbf{A}}\right)\left(\mathbf{H}'_{\mathrm{DL}}\hat{\mathbf{A}}\right)^H\right] \\ &+ \alpha \Re\mathrm{tr}\left[(\mathbf{H}_{\mathrm{DL}}\hat{\mathbf{A}} - \mathbf{I})(\mathbf{H}''_{\mathrm{DL}}\hat{\mathbf{A}})^H\right] \\ &+ \frac{N_0 N_U}{P_T}\mathrm{tr}\left[\hat{\mathbf{A}}\hat{\mathbf{A}}^H\right] \\ &+ j\mathrm{tr}\left[\mathbf{\Psi}^T(\mathbf{H}_{\mathrm{DL}}\hat{\mathbf{A}} - \mathbf{H}^*_{\mathrm{DL}}\hat{\mathbf{A}}^*)\right].\end{aligned}$$

Setting the derivative of L with respect to $\hat{\mathbf{A}}$ to $\mathbf{0}$ yields

$$\hat{\mathbf{A}} = \left(\mathbf{H}_{\mathrm{DL}}^H\mathbf{H}_{\mathrm{DL}} + \alpha\mathbf{H}'^H_{\mathrm{DL}}\mathbf{H}'_{\mathrm{DL}} + \frac{\alpha}{2}\left(\mathbf{H}_{\mathrm{DL}}^H\mathbf{H}''_{\mathrm{DL}} + \mathbf{H}''^H_{\mathrm{DL}}\mathbf{H}_{\mathrm{DL}}\right) + \frac{N_0 N_U}{P_T}\mathbf{I}_N\right)^{-1}\left(j\mathbf{H}_{\mathrm{DL}}^H\mathbf{\Psi} + \mathbf{H}_{\mathrm{DL}}^H + \frac{\alpha}{2}\mathbf{H}''^H_{\mathrm{DL}}\right), \tag{9}$$

where the value of $\mathbf{\Psi}$ is fixed thanks to the constraint $\Im(\mathbf{H}_{\mathrm{DL}}\mathbf{A}) = \mathbf{0}$. Denoting $\mathbf{X} = \mathbf{H}_{\mathrm{DL}}^H\mathbf{H}_{\mathrm{DL}} + \frac{\alpha}{2}\left[\mathbf{H}_{\mathrm{DL}}^H\mathbf{H}_{\mathrm{DL}}'' + \mathbf{H}_{\mathrm{DL}}''^H\mathbf{H}_{\mathrm{DL}}\right] + \alpha\mathbf{H}_{\mathrm{DL}}'^H\mathbf{H}_{\mathrm{DL}}' + \frac{N_0 N_U}{P_T}\mathbf{I}_N$, we find

$$\mathbf{\Psi} = -\left(\Re\left(\mathbf{H}_{\mathrm{DL}}\mathbf{X}^{-1}\mathbf{H}_{\mathrm{DL}}^H\right)\right)^{-1}\Im(\mathbf{H}_{\mathrm{DL}}\mathbf{X}^{-1}(\mathbf{H}_{\mathrm{DL}}^H + \frac{\alpha}{2}\mathbf{H}_{\mathrm{DL}}''^H)).$$

C. Complexity of computation of the proposed precoders and decoders

Table II gives an order of complexity of computing the proposed optimized designs with respect to classical designs. By classical designs, we mean precoders and decoders that rely on the hypothesis of channel frequency flatness at the subcarrier level, i.e., $\mathbf{H}'(\omega_m) = \mathbf{H}''(\omega_m) = \mathbf{0}$. For the calculation, only matrix multiplications and inversions are taken into account given that they are the most complex operations. It is assumed that for general matrices $\mathbf{D} \in \mathbb{C}^{l\times m}, \mathbf{E} \in \mathbb{C}^{m\times n}, \mathbf{F} \in \mathbb{C}^{m\times m}$, performing matrix multiplication $\mathbf{DE}$ has complexity $O(lmn)$ and matrix inversion $\mathbf{F}^{-1}$ has complexity $O(m^3)$. One can check that the calculation complexity of the optimized designs remains similar to the classical. Note that the designs in DL are more complex since they require one more matrix multiplication for the calculation of ξ_{DL}. Furthermore, the opt. MMSE precoder is slightly more complex than the opt. MMSE decoder due to the required calculation of $\mathbf{\Psi}$.

IV. Simulation Results

The following simulations first aim at demonstrating the accuracy of the derived asymptotic MSE expression in practical situations. Secondly, they validate the performance of the optimized precoders and decoders w.r.t. classical precoder and decoder designs. A FBMC-OQAM system is considered with $2M = 128$ subcarriers and subcarrier spacing 15kHz as in LTE. The channels are randomly drawn from the ITU Vehicular A or B channel model, *i.e.* a mildly or highly frequency selective channel respectively. Furthermore, they remain constant during the frame transmission (quasi-static assumption). The Phydyas prototype pulse with overlapping factor $\kappa = 4$ is used in the simulations [18]. This pulse does not fully satisfy the PR constraints but is of the near-perfect-reconstruction (NPR) type. Given that it almost fulfills PR constraints, the derived MSE expression (1) remains a very good approximation of the distortion, as will be shown in the following.

Fig. 4 shows the MSE of the classical and optimized MMSE decoders for a specific channel realization. The channel model simulated is the Vehicular B channel. The BS is assumed to have $N = 4$ antennas serving $N_U = 2$ users and the SNR of the system is 25dB. One can first check that the simulated MSE (in cross markers) perfectly matches the theoretical approximation (in solid line) of (1). Furthermore, in the high SNR regime considered here, the classical MMSE decoder is limited by the distortion induced by the channel frequency selectivity. On the other hand, the optimized MMSE decoder uses the two extra antennas to cancel the distortion, giving a clear gain of performance.

In Fig. 5 and Fig. 6, the symbol error rate (SER) for the classical and optimized decoders are plotted for a fixed number of users $N_U = 3$ and different number of BS antennas N. The signal constellation is a 16-QAM.

In Fig. 5, the Veh. A channel model is considered and the classical decoders can achieve the same performance as the optimized ones. This comes from the fact that the assumption of an approximately flat channel inside each subchannel is accurate. On the other hand, in Fig. 6, the Veh. B channel model is considered, i.e., a highly selective channel. The SER saturates very quickly with a classical decoder while the optimized ZF or MMSE decoder can compensate for the distortion as the number of BS antennas N grows and the SER therefore saturates at higher SNR. In the case $N_U = 3, N = 6$, the SER does not even saturate in the considered SNR range since the BS has twice as many antennas and can completely remove the first order approximation of the distortion. This is in accordance with the asymptotic study at high SNR conducted in Section III-A3. As expected, the MMSE designs outperform the ZF designs, and this gain is larger for a small number of BS antennas. Indeed, as the number of BS antennas increases, the interference can be better handled and the regularization gain of the MMSE decoder is reduced.

In Fig. 7, a 4-QAM constellation and the Veh. B channel model are considered in the UL. The proposed decoder designs are compared with a 3-tap frequency sampling equalizer that follows the design of [9] with target frequency points chosen according to a ZF criterion. One can check that the 3-tap equalizer has a gain of performance relative to the proposed designs for the same antenna configuration. Note however that the multi-tap design has a much larger complexity in terms of hardware implementation and calculation of the equalizer coefficients. Moreover, it adds a reconstruction delay to the demodulation chain.

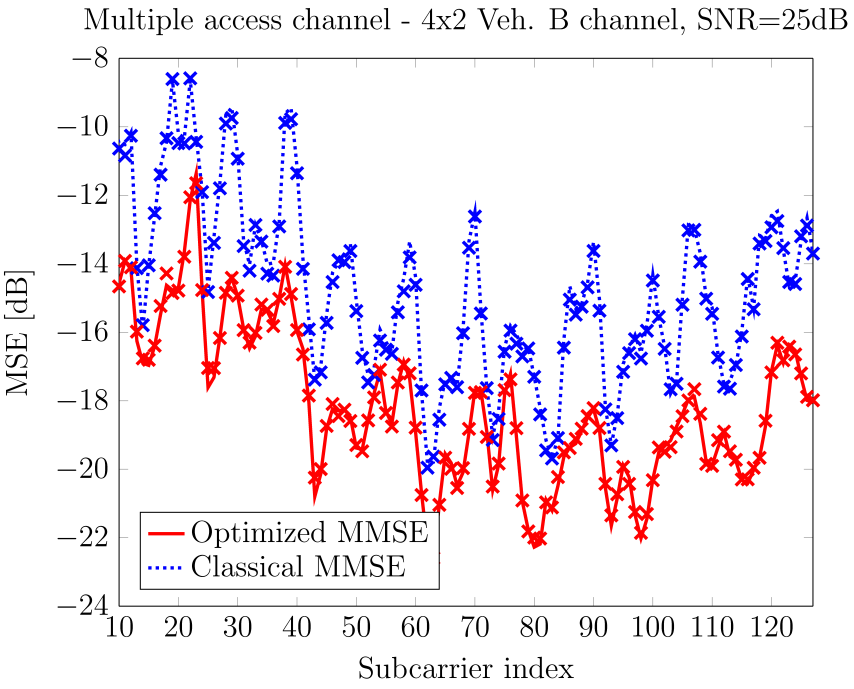

Fig. 4. The optimized MMSE decoder clearly outperforms the classical MMSE decoder. The asymptotic approximation of the MSE represented in a solid line matches perfectly the simulated MSE in crosses.

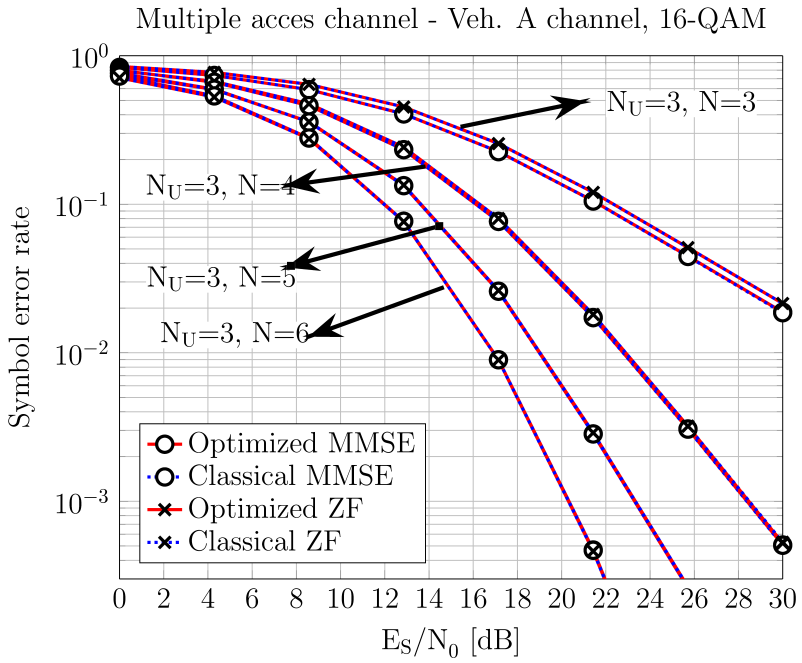

Fig. 5. SER of the optimized and classical ZF/MMSE decoders and Veh. A channel model.

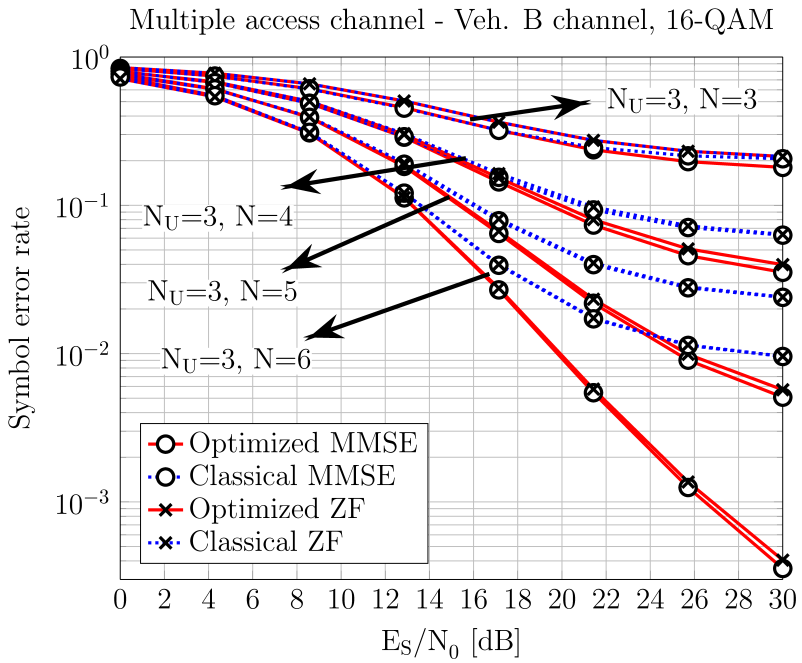

Fig. 6. SER of the optimized and classical ZF/MMSE decoder and Veh. B channel model

Fig. 8 has exactly the same simulation parameters as Fig. 7 but for the DL. One can check that the performance of the ZF precoder in DL is similar to the decoder one in UL. Note that the SER performances of the precoder and decoder might differ. Indeed, even though the MSE expression is dual in UL and in DL, the distribution of the

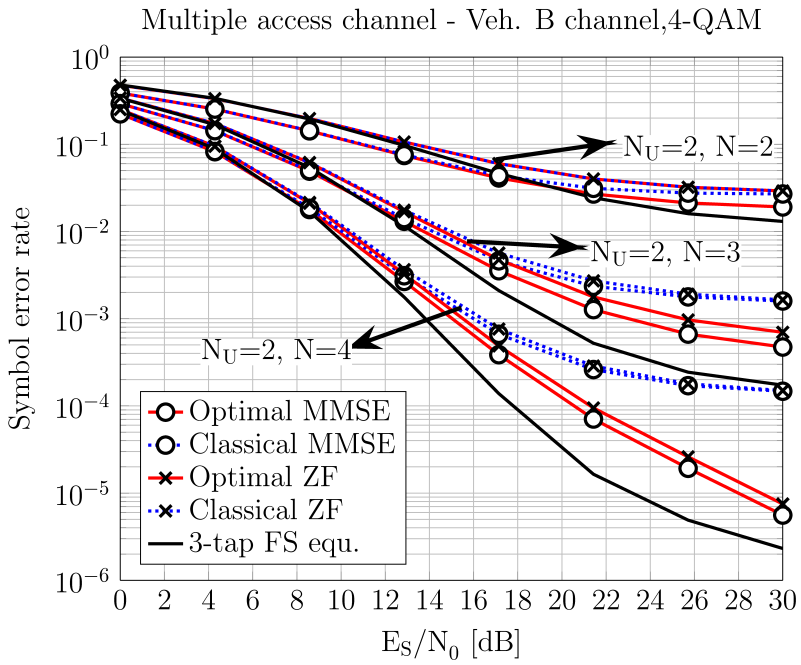

Fig. 7. SER of the optimized and classical ZF/MMSE decoder and a 3-tap frequency sampling equalizer.

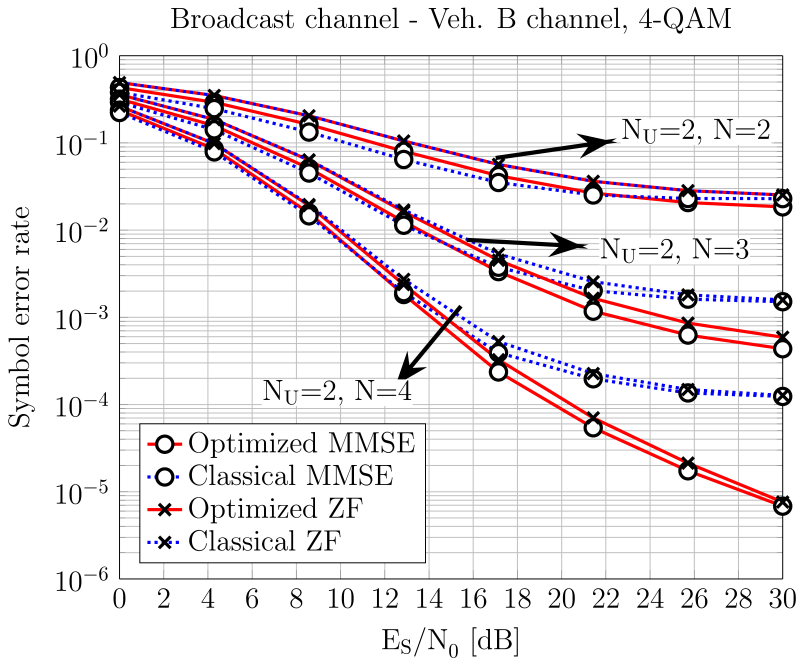

Fig. 8. SER of the optimized, classical ZF/MMSE precoder.

per-stream SER might differ due to the correlation of the noise arising in UL but not in DL. Moreover, due to the ZF constraint on $\Im(\mathbf{H}_{\mathrm{DL}}\mathbf{A}_{\mathrm{DL}}^{\mathrm{MMSE}}) = 0$, the optimized MMSE precoder performs slightly worse than the classical

MMSE precoder at low SNR.

V. Conclusion

This paper investigated the design of optimized FBMC-OQAM precoders and decoders for a MU MIMO scenario highly selective channel. The asymptotic expression of the MSE of a FBMC transceiver was recalled, simplified and generalized. Optimizing the MSE expression, expressions of the optimized linear precoder and decoder were found under either a ZF criterion or a MMSE criterion. As soon as the BS has more antennas than the number of users, the optimized structures use those extra degrees of freedom to compensate for the distortion induced by channel frequency selectivity. From an asymptotic study at high SNR, it was shown that the first order approximation of the distortion can even be completely removed if the BS has at least twice as many antennas as the number of users. Simulation results have demonstrated the accuracy of the new asymptotic expression of the distortion as well as the performance of the optimized precoders and decoders.

Appendix A
Distortion expression

In this appendix, we are interested only in the intrinsic distortion caused by the FBMC signal itself in the presence of channel frequency selectivity. Since the additive noise samples are assumed to be uncorrelated with the signal of interest, we will assume a noise-free received signal. In order to derive the distortion expression, we will first define different notations and recall one Lemma of [16].

We define $\mathbf{y}_{l_0,m_0}^{p,q} \in \mathbb{C}^{S\times 1}$ as

$$\mathbf{y}_{l_0,m_0}^{p,q} = \sum_{l=0}^{2N_s-1}\sum_{m=0}^{2M-1} \mathbf{d}_{l,m} \sum_{n=0}^{L_q-1} p_{l,m}[n] q_{l_0,m_0}^{*}[n].$$

The symbols $\mathbf{y}_{l_0,m_0}^{p,q}$ can be seen as the complex demodulated samples at subcarrier m_0 and multicarrier symbol l_0, before de-staggering, if the real-valued symbols streams $\mathbf{d}_{l,m}$ are FBMC/OQAM modulated using a prototype pulse $p[n]$ and demodulated using a prototype pulse $q[n]$ and for an ideal channel, i.e., $\mathbf{H}(\omega) = \mathbf{I}_S$. Moreover, if p and q are perfect reconstruction (bi-orthogonal) pulses, one will have $\mathbf{d}_{l_0,m_0} = \Re(\mathbf{y}_{l_0,m_0}^{p,q})$.

As detailed in Section II-A, to compensate for the effect of the channel, a single-tap precoding matrix $\mathbf{A}(\omega)$ and decoding matrix $\mathbf{B}(\omega)$ are used, operating at the per-subcarrier level. At the transmitter, the symbols $\mathbf{d}_{l,m}$ are precoded by matrix $\mathbf{A}(\omega_m)$. At the receiver, the equalized symbols are denoted by $\mathbf{x}_{l_0,m_0}^{p,q} = \mathbf{B}(\omega_{m_0})\mathbf{z}_{l_0,m_0}^{p,q}$ where $\mathbf{z}_{l_0,m_0}^{p,q}$ are the demodulated symbols at the receiver before decoding, i.e.,

$$\mathbf{z}_{l_0,m_0}^{p,q} = \sum_{n=0}^{L_q-1} \mathbf{r}[n] q_{l_0,m_0}^{*}[n].$$

Note that one does not necessarily have $\Re(\mathbf{x}_{l_0,m_0}^{p,q}) = \mathbf{d}_{l_0,m_0}$ even if $\mathbf{B}(\omega)\mathbf{H}(\omega)\mathbf{A}(\omega) = \mathbf{I}_S$ (and if no additive noise is present) due to the fact that the FBMC-OQAM orthogonality does not hold anymore if the channel is not exactly flat. However, this will hold approximately if all frequency-depending quantities, $\mathbf{B}(\omega), \mathbf{H}(\omega), \mathbf{A}(\omega)$, are sufficiently flat as functions of ω provided that $\mathbf{B}(\omega)\mathbf{H}(\omega)\mathbf{A}(\omega) = \mathbf{I}_S$. Our objective is to find an approximate

expression for the associated error. This was already done in [16] but for the special case of ZF (channel inversion), i.e.,

$$\mathbf{B}(\omega)\mathbf{H}(\omega)\mathbf{A}(\omega) = \mathbf{I}_S.$$

We here extend and greatly simplify the formula derived in [16] to the general case of non channel inversion, i.e.,

$$\mathbf{B}(\omega)\mathbf{H}(\omega)\mathbf{A}(\omega) \neq \mathbf{I}_S.$$

To derive the result of Theorem II.1, we will use the following result, proven in [16]. We will basically assume that all frequency depending quantities are smooth functions of ω and that the prototype pulses are sampled versions of smooth analog waveforms, namely, $(\mathbf{As1})$-$(\mathbf{As3})$.

Lemma 1. *Under assumptions* $(\mathbf{As1})$-$(\mathbf{As3})$*, we have*

$$\begin{aligned}&\mathbf{z}_{l_0,m_0}^{p,q}\\ &= \sum_{k=0}^{R}\sum_{k'=0}^{R-k}\frac{(-j)^{k+k'}}{(2M)^{k+k'}k!k'!}\mathbf{H}^{(k)}\mathbf{A}^{(k')}\mathbf{y}_{l_0,m_0}^{p,q^{(k)}}(k') + O(M^{-R})\end{aligned}$$

where

$$\mathbf{y}_{l_0,m_0}^{p,q^{(k)}}(k') = \sum_{r=0}^{k'}\frac{k'!}{r!(k'-r)!}(-1)^r\mathbf{y}_{l_0,m_0}^{p^{(r)},q^{(k+k'-r)}}$$

and where $p^{(r)}, q^{(r)}$ *are the sampled versions of the* r*-th time domain derivatives of the original prototype pulses. Superscript* $^{(k)}$ *denotes the m-th order derivative of the corresponding frequency dependent quantity, which always is evaluated at subcarrier* m_0 *(here and in the following of the appendix).*

A direct application of the above lemma for $R = 2$ allows us to write

$$\mathbf{x}_{l_0,m_0}^{p,q} = \mathbf{BHA}\mathbf{y}_{l_0,m_0} - \frac{j}{2M}\boldsymbol{\epsilon}_1 - \frac{1}{2(2M)^2}\boldsymbol{\epsilon}_2 + O(M^{-2}) \tag{10}$$

where we have defined

$$\begin{aligned}\boldsymbol{\epsilon}_1 &= \mathbf{B}(\mathbf{HA})^{(1)}\mathbf{y}_{l_0,m_0}^{p,q^{(1)}} - \mathbf{BHA}^{(1)}\mathbf{y}_{l_0,m_0}^{p^{(1)},q}\\ \boldsymbol{\epsilon}_2 &= \mathbf{B}(\mathbf{HA})^{(2)}\mathbf{y}_{l_0,m_0}^{p,q^{(2)}} - 2\mathbf{B}\left(\mathbf{HA}^{(1)}\right)^{(1)}\mathbf{y}_{l_0,m_0}^{p^{(1)},q^{(1)}}\\ &\quad + \mathbf{BHA}^{(2)}\mathbf{y}_{l_0,m_0}^{p^{(2)},q}\end{aligned}$$

At this point, force $p = q$ so that the same prototype pulse is used at both transmitter and receiver. We define the distortion error associated with the complex-valued symbols as[4]

$$P_d(m) = 2\mathbb{E}\left(\|\Re(\mathbf{x}_{l_0,m_0}^{p,q}) - \mathbf{d}_{l_0,m_0}\|^2\right). \tag{11}$$

[4]Note that this definition is in accordance with equation (1) when noise is absent.

We now need to define some pulse-related quantities. Given two generic pulses, p, q of length $2M\kappa$ and let $\mathbf{P}$ and $\mathbf{Q}$ denote two $2M \times \kappa$ matrices obtained by arranging the samples of the respective pulses in columns from left to right. We will define

$$\mathcal{R}(p,q) = \mathbf{P} \circledast \mathbf{J}_{2M}\mathbf{Q}$$
$$\mathcal{S}(p,q) = (\mathbf{J}_2 \otimes \mathbf{I}_M)\,\mathbf{P} \circledast \mathbf{J}_{2M}\mathbf{Q}$$

where $\circledast$ denotes row-wise convolution, $\otimes$ denotes Kronecker product, $\mathbf{I}_M$ (resp. $\mathbf{J}_M$) are the identity (resp. exchange) matrices of order M. Given four generic pulses p, q, r, s, we define

$$\begin{aligned}
&\eta^{\pm}(p,q,r,s)\\
&= \frac{1}{2M}\text{tr}\left[\mathbf{U}^{+}\mathcal{R}(p,q)\,\mathcal{R}^{T}(r,s) + \mathbf{U}^{-}\mathcal{S}(p,q)\,\mathcal{S}^{T}(r,s)\right]\\
&\eta^{\mp}(p,q,r,s)\\
&= \frac{1}{2M}\text{tr}\left[\mathbf{U}^{-}\mathcal{R}(p,q)\,\mathcal{R}^{T}(r,s) + \mathbf{U}^{+}\mathcal{S}(p,q)\,\mathcal{S}^{T}(r,s)\right]
\end{aligned}$$

where $\mathbf{U}^{\pm} = \mathbf{I}_2 \otimes (\mathbf{I}_M \pm \mathbf{J}_M)$. In order to simplify the notations, given four integers m, n, r, s, we will define $\eta_{mnrs}^{(+,-)} = \eta^{\pm}\left(p^{(m)}, p^{(n)}, p^{(r)}, p^{(s)}\right)$.

Assuming that the pulse has PR properties $(\mathbf{As2})$ so that $\mathbf{d}_{l_0,m_0} = \Re(\mathbf{y}_{l_0,m_0}^{p,q})$, we can obtain an asymptotic expression for this distortion by simply inserting (10) in (11) for $p = q$ and by using the fact that [3, Appendix B]

$$\begin{aligned}
\mathbb{E}\left(\Re(\mathbf{y}_{l_0,m_0}^{p^{(m)},q^{(n)}})\Re^{T}(\mathbf{y}_{l_0,m_0}^{p^{(r)},q^{(s)}})\right) &= \eta_{mnrs}^{(+,-)}\mathbf{I}_S\\
\mathbb{E}\left(\Im(\mathbf{y}_{l_0,m_0}^{p^{(m)},q^{(n)}})\Im^{T}(\mathbf{y}_{l_0,m_0}^{p^{(r)},q^{(s)}})\right) &= \eta_{mnrs}^{(-,+)}\mathbf{I}_S\\
\mathbb{E}\left(\Re(\mathbf{y}_{l_0,m_0}^{p^{(m)},q^{(n)}})\Im^{T}(\mathbf{y}_{l_0,m_0}^{p^{(r)},q^{(s)}})\right) &= \mathbf{0}.
\end{aligned}$$

The resulting expression can be more compactly expressed by using the fact that $\eta_{mnrs}^{(+,-)} = \eta_{rsmn}^{(+,-)}$, $\eta_{mnrs}^{(+,-)} = \eta_{nmsr}^{(+,-)}$,[5] as established in Lemma 2 of Appendix B. Furthermore, if we assume that the prototype pulse is either symmetric or anti-symmetric, one can establish that $\eta_{0000}^{(+,-)} = \eta_{0000}^{(-,+)}$, $\eta_{0001}^{(+,-)} = \eta_{0001}^{(-,+)}$, $\eta_{0101}^{(+,-)} = \eta_{0101}^{(-,+)}$ and $\eta_{0020}^{(+,-)} = \eta_{0020}^{(-,+)}$, a fact that is proven in Lemma 3 of Appendix B. If, additionally, the prototype pulse meets the PR conditions, we can guarantee that $\eta_{0001}^{(+,-)} = 0$ as established in Lemma 4 of Appendix B.

Using all this, together with the fact that

$$\begin{aligned}
\text{tr}\left[\Re(\mathbf{X})\Re^{T}(\mathbf{Y}) + \Im(\mathbf{X})\Im^{T}(\mathbf{Y})\right] &= \Re\text{tr}\left[\mathbf{X}\mathbf{Y}^{H}\right]\\
\text{tr}\left[\Im(\mathbf{X})\Re^{T}(\mathbf{Y}) - \Re(\mathbf{X})\Im^{T}(\mathbf{Y})\right] &= \Im\text{tr}\left[\mathbf{X}\mathbf{Y}^{H}\right]
\end{aligned}$$

for any complex valued matrices $\mathbf{X}$, $\mathbf{Y}$ of appropriate dimensions, we see that

$$P_d(m) = 2\xi_{0,m} + \frac{2}{(2M)^2}\xi_{2,m} + O\left(M^{-2}\right) \tag{12}$$

[5]Obviously, the same identities hold if $(+,-)$ is replaced by $(-,+)$.

where we have defined

$$\begin{aligned}
\xi_{0,m} &= \eta_{0000}^{(+,-)}\text{tr}\left[\left(\mathbf{BHA}-\mathbf{I}\right)\left(\mathbf{BHA}-\mathbf{I}\right)^{H}\right] \\
\xi_{2,m} &= \eta_{1010}^{(+,-)}\left(\text{tr}\left[\mathbf{BHA}^{(1)}\left(\mathbf{BHA}^{(1)}\right)^{H}\right]+\text{tr}\left[\mathbf{B}\left(\mathbf{HA}\right)^{(1)}\left(\mathbf{B}\left(\mathbf{HA}\right)^{(1)}\right)^{H}\right]\right) \\
&\quad-\eta_{2000}^{(+,-)}\left(\Re\text{tr}\left[\left(\mathbf{BHA}-\mathbf{I}\right)\left(\mathbf{BHA}^{(2)}\right)^{H}\right]+\Re\text{tr}\left[\left(\mathbf{BHA}-\mathbf{I}\right)\left(\mathbf{B}\left(\mathbf{HA}\right)^{(2)}\right)^{H}\right]\right) \\
&\quad+2\eta_{0011}^{(+,-)}\text{tr}\left[\Re\left[\mathbf{BHA}-\mathbf{I}\right]\Re^{T}\left[\mathbf{B}\left(\mathbf{HA}^{(1)}\right)^{(1)}\right]\right] \\
&\quad+2\eta_{0011}^{(-,+)}\text{tr}\left[\Im\left[\mathbf{BHA}-\mathbf{I}\right]\Im^{T}\left[\mathbf{B}\left(\mathbf{HA}^{(1)}\right)^{(1)}\right]\right] \\
&\quad-2\eta_{1001}^{(+,-)}\text{tr}\left[\Im\left[\mathbf{B}\left(\mathbf{HA}\right)^{(1)}\right]\Im^{T}\left[\mathbf{BHA}^{(1)}\right]\right] \\
&\quad-2\eta_{1001}^{(-,+)}\text{tr}\left[\Re\left[\mathbf{B}\left(\mathbf{HA}\right)^{(1)}\right]\Re^{T}\left[\mathbf{BHA}^{(1)}\right]\right]
\end{aligned}$$

and where all frequency-depending matrices are evaluated at $\omega=\omega_m$.

It is easy to see that, thanks to the PR property of the prototype pulse, we will have $\eta_{0000}^{(+,-)}=P_s/2$, where we recall that P_s is the power of the complex constellation symbols. Therefore, the asymptotic distortion power depends on six different pulse-related quantities, which present some non-trivial interrelationships. To establish these interrelationships, we invoke again Lemma 3 of Appendix B. In particular, the relationships in (17)-(18) allow us to establish

$$\left[\eta_{1001}^{(+,-)}-\eta_{1001}^{(-,+)}\right]-\left[\eta_{0011}^{(+,-)}-\eta_{0011}^{(-,+)}\right]=0 \tag{13}$$

$$\eta_{0011}^{(+,-)}+\eta_{1010}^{(+,-)}=0. \tag{14}$$

We can find further equivalences between the different pulse quantities by considering here the asymptotic domain as $M\to\infty$ together with the fact that the prototype pulse is, by assumption, a sampled version of a smooth analog waveform.

Indeed, applying the result in Proposition B.1, Corollary 1 and Lemma 6 in Appendix B together with the fact that the prototype pulse is symmetric and PR compliant, we obtain

$$\eta_{2000}^{(+,-)}-\eta_{0011}^{(+,-)}+\eta_{1010}^{(+,-)}-\eta_{1001}^{(-,+)}=O(M^{-1}) \tag{15}$$

$$\eta_{0011}^{(+,-)}-\eta_{2000}^{(+,-)}=O(M^{-2}). \tag{16}$$

We may consider the system of equations formed by (13),(14),(15) and (16). Denoting $\alpha=\eta_{1010}^{(+,-)}$ and $\beta=\eta_{0011}^{(-,+)}$, we can express the system of equations as

$$\begin{bmatrix} 1 & -1 & -1 & 0 \\ 0 & 0 & 1 & 0 \\ 0 & -1 & -1 & 1 \\ 0 & 0 & 1 & -1 \end{bmatrix}\begin{bmatrix} \eta_{1001}^{(+,-)} \\ \eta_{1001}^{(-,+)} \\ \eta_{0011}^{(+,-)} \\ \eta_{2000}^{(+,-)} \end{bmatrix}=\begin{bmatrix} -\beta \\ -\alpha \\ -\alpha \\ 0 \end{bmatrix}+O(M^{-1})$$

so that we can conclude that

$$\begin{bmatrix} \eta_{1001}^{(+,-)} \\ \eta_{1001}^{(-,+)} \\ \eta_{0011}^{(+,-)} \\ \eta_{2000}^{(+,-)} \end{bmatrix} = \begin{bmatrix} -\beta \\ \alpha \\ -\alpha \\ -\alpha \end{bmatrix} + O(M^{-1})$$

Using this in (12) we obtain (2).

APPENDIX B
SOME PROPERTIES OF THE QUANTITIES $\eta_{mnrs}^{(+,-)}$

In this appendix, we provide some identities on the quantities $\eta_{mnrs}^{(+,-)}$, $\eta_{mnrs}^{(-,+)}$ that will clearly simplify the expression for the asymptotic distortion derived above. We will begin by presenting some properties that hold exactly for all values of M.

A. Non-asymptotic properties

Let us begin with general properties that hold regardless of whether the pulses are symmetric or not.

Lemma 2. *By the definition of the $\eta^{\pm}(p,q,r,s)$, and regardless of the pulse symmetries, we have*

$$\eta^{\pm}(p,q,r,s) = \eta^{\pm}(r,s,p,q)$$

and

$$\eta^{\pm}(p,q,r,s) = \eta^{\pm}(q,p,s,r).$$

The same identities hold if $\pm$ is replaced by $\mp$ everywhere.

Proof: Indeed, the first result is a consequence of the fact that

$$\left(\mathbf{U}^{\pm}\mathcal{R}(p,q)\,\mathcal{R}^T(r,s)\right)^T = \mathcal{R}(r,s)\,\mathcal{R}^T(p,q)\,\mathbf{U}^{\pm}$$
$$\left(\mathbf{U}^{\pm}\mathcal{S}(p,q)\,\mathcal{S}^T(r,s)\right)^T = \mathcal{S}(r,s)\,\mathcal{S}^T(p,q)\,\mathbf{U}^{\pm}$$

whereas the second one follows from the identities

$$\mathcal{R}(p,q)\,\mathcal{R}^T(r,s) = \mathbf{J}_{2M}\mathcal{R}(q,p)\,\mathcal{R}^T(s,r)\,\mathbf{J}_{2M},$$
$$\mathcal{S}(p,q)\,\mathcal{S}^T(r,s) = (\mathbf{I}_2 \otimes \mathbf{J}_M)\,\mathcal{S}(q,p)\,\mathcal{S}^T(s,r)\,(\mathbf{I}_2 \otimes \mathbf{J}_M)$$

and the definition of $\mathbf{U}^{\pm}$. ■

Sometimes, it is useful to consider a relationship between quantities of the type $\eta^{\pm}$ and $\eta^{\mp}$. In order to obtain such relationships, we impose that the pulses are either symmetric or anti-symmetric in the time domain.

Lemma 3. *Assume that all the pulses p, q, r, s are either symmetric or anti-symmetric in the time domain. Let $s(p)$ be defined so that $s(p) = 0$ if the pulse p has even symmetry and $s(p) = 1$ if the pulse is anti-symmetric. Then, we can write*

$$\begin{aligned}&(-1)^{s(p)}\left[\eta^{\pm}(p,q,r,s) - \eta^{\mp}(p,q,r,s)\right]\\&+ (-1)^{s(r)}\left[\eta^{\pm}(r,q,p,s) - \eta^{\mp}(r,q,p,s)\right] = 0\end{aligned} \tag{17}$$

and also

$$\begin{aligned}&(-1)^{s(p)}\left[\eta^{\pm}(p,q,r,s) + \eta^{\mp}(p,q,r,s)\right]\\&\pm (-1)^{s(p)}\left[\eta^{\pm}(p,q,s,r) - \eta^{\mp}(p,q,s,r)\right]\\&= (-1)^{s(s)}\left[\eta^{\pm}(s,q,r,p) + \eta^{\mp}(s,q,r,p)\right]\end{aligned} \tag{18}$$

In particular, for the specific case where $p = r$ we have

$$\eta^{\pm}(p,q,p,s) = \eta^{\mp}(p,q,p,s).$$

Finally, if $q = s$ and the pulses p and r have the same type of symmetry, we have

$$\eta^{\pm}(p,q,r,q) = \eta^{\mp}(p,q,r,q).$$

Proof: Let us denote by $\mathcal{R}_1(p,q)$ and $\mathcal{R}_2(p,q)$ the upper and lower matrices of $\mathcal{R}(p,q)$, and equivalently for $\mathcal{S}_1(p,q)$ and $\mathcal{S}_2(p,q)$. Let $\mathbf{P}$ denote a $2M \times \kappa$ matrix obtained by arranging the pulse $p[n]$ in columns, and let $\mathbf{P}_1$ and $\mathbf{P}_2$ respectively denote the matrices obtained by selecting the M upper and lower rows of $\mathbf{P}$ respectively. By the symmetry of $p[n]$, we know that

$$\mathbf{P}_1 = (-1)^{s(p)}\mathbf{J}_M\mathbf{P}_2\mathbf{J}_{2\kappa-1}.$$

On the other hand, we can prove that, for any four matrices $\mathbf{A}, \mathbf{B}, \mathbf{C}$ and $\mathbf{D}$ of dimensions $M \times \kappa$, the diagonal entries of $(\mathbf{A} \circledast \mathbf{B}\mathbf{J}_\kappa)(\mathbf{C} \circledast \mathbf{D}\mathbf{J}_\kappa)^T \mathbf{J}_M$ are equal to the diagonal entries of $\mathbf{J}_M(\mathbf{C} \circledast \mathbf{J}_M\mathbf{B})(\mathbf{A} \circledast \mathbf{J}_M\mathbf{D})^T$. This shows that, using pulse symmetry,

$$\begin{aligned}\text{tr}\left[\mathcal{R}_1(p,q)\mathcal{R}_1^T(r,s)\mathbf{J}_M\right] &= \text{tr}\left[\mathbf{J}_M(\mathbf{J}_M\mathbf{P}_1 \circledast \mathbf{Q}_2)(\mathbf{J}_M\mathbf{R}_1 \circledast \mathbf{S}_2)^T\right]\\&= (-1)^{s(p)+s(r)}\,\text{tr}\left[(\mathbf{P}_2\mathbf{J}_\kappa \circledast \mathbf{Q}_2)(\mathbf{R}_2\mathbf{J}_\kappa \circledast \mathbf{S}_2)^T\mathbf{J}_M\right]\\&\overset{(*)}{=} (-1)^{s(p)+s(r)}\,\text{tr}\left[\mathbf{J}_M(\mathbf{S}_2 \circledast \mathbf{J}_M\mathbf{P}_2)(\mathbf{Q}_2 \circledast \mathbf{J}_M\mathbf{R}_2)^T\right]\\&= (-1)^{s(p)+s(r)}\,\text{tr}\left[\mathbf{J}_M(\mathbf{P}_2 \circledast \mathbf{J}_M\mathbf{S}_2)(\mathbf{R}_2 \circledast \mathbf{J}_M\mathbf{Q}_2)^T\right]\\&= (-1)^{s(p)+s(r)}\,\text{tr}\left[\mathbf{J}_M\mathcal{S}_1(p,s)\mathcal{S}_1^T(r,q)\right]\\&= (-1)^{s(p)+s(r)}\,\text{tr}\left[\mathbf{J}_M\mathcal{S}_1(r,q)\mathcal{S}_1^T(p,s)\right]\end{aligned} \tag{19}$$

where the identity in $(*)$ follows from the above convolution result. Equivalently, we will obviously have

$$\text{tr}\left[\mathcal{R}_2(p,q)\mathcal{R}_2^T(r,s)\mathbf{J}_M\right] = (-1)^{s(p)+s(r)}\,\text{tr}\left[\mathbf{J}_M\mathcal{S}_2(r,q)\mathcal{S}_2^T(p,s)\right]$$

and the two above identities directly prove (17). Regarding the identity in (18), it follows easily from the above identities together with the fact that $\mathbf{J}_M \mathcal{R}_i(p,q) = \mathcal{R}_{3-i}(q,p)$, $\mathbf{J}_M \mathcal{S}_i(p,q) = \mathcal{S}_i(q,p)$, $i = 1, 2$, and the fact that

$$\text{tr}\left[\mathcal{R}_1(p,q)\,\mathcal{R}_2^T(r,s)\,\mathbf{J}_M\right] = (-1)^{s(p)+s(r)}\,\text{tr}\left[\mathcal{R}_1(r,q)\,\mathcal{R}_2^T(p,s)\,\mathbf{J}_M\right]$$
$$\text{tr}\left[\mathcal{S}_1(p,q)\,\mathcal{S}_2^T(r,s)\,\mathbf{J}_M\right] = (-1)^{s(p)+s(r)}\,\text{tr}\left[\mathcal{S}_1(r,q)\,\mathcal{S}_2^T(p,s)\,\mathbf{J}_M\right]$$

which can be established following the same approach as in (19). The last two identities in the statement of the lemma are obtained as special cases of (17). ■

We finalize the description of the non-asymptotic properties of the $\eta^{\pm}(p,q,r,s)$ with a result that will be useful whenever two of the pulses meet the perfect reconstruction conditions.

Lemma 4. *Assume that the two pulses p, q meet the perfect reconstruction conditions, and that r and s are either symmetric or anti-symmetric in the time domain and have the opposite symmetry. Then $\eta^{\pm}(p,q,r,s) = 0$.*

Proof: Since p, q have PR conditions, we know that $\mathbf{U}^{-}\mathcal{S}(p,q)$ is an all-zero matrix whereas $\mathbf{U}^{+}\mathcal{R}(p,q)$ has zeros everywhere except for the central column, which is filled with 1s. Therefore, we are able to write

$$\eta^{\pm}(p,q,r,s) = \frac{1}{2M}\sum_{n=1}^{2M\kappa} r[n]s[2M\kappa - n + 1] = 0$$

where the last equality follows from the fact that r and s have the opposite symmetry. ■

B. Asymptotic properties

Let us now consider some properties of the $\eta^{\pm}(p,q,p,s)$ that are obtained by assuming that the pulses are sampled versions of a smooth analog waveform. In other words, we assume that $p[n]$, $q[n]$, $r[n]$ and $s[n]$ are sampled versions of the waveforms $p(t), q(t), r(t)$ and $s(t)$ respectively, according to the properties in $(\mathbf{As2})$. This means that we can express

$$p[n] = p\left(\left(n - \frac{N+1}{2}\right)\frac{T_s}{2M}\right)$$

where $p(t)$ has the usual properties in $(\mathbf{As2})$. The same holds for the rest of the pulses.

Let us denote $p_m[n]$ the m-th polyphase component of $p[n]$, which can be expressed as

$$p_m[n] = p_m\left(\left(n - \frac{1}{2}\right)\frac{T_s}{2M}\right)$$

where $p_m(t)$ is the m-th section of $p(t)$, namely

$$p_m(t) = p\left(t - \left(m + \frac{\kappa}{2} - 1\right)T_s\right)$$

which has support $[0, T_s]$. The definition of $p_m(t)$ is only valid for $m = 1, \ldots, \kappa$, but we will consider $p_m(t) = 0$ for values of m outside this range. The same definitions carry over to the other pulses, namely q, r and s.

With all these definitions, we are now in a position to establish the first asymptotic result associated with $\eta^{\pm}(p,q,p,s)$. The following result asymptotically relates the original quantity $\eta^{\pm}(p,q,p,s)$ with an equivalent definition that is constructed using the analog waveforms instead of the sampled ones.

Lemma 5. *Under the above assumptions, we can write*

$$\eta^{\pm}(p,q,r,s) = \bar{\eta}^{\pm}(p,q,r,s) + O(M^{-2})$$

where

$$\bar{\eta}^{\pm}(p,q,r,s) = \sum_{\ell=1}^{2\kappa-1}\sum_{m=1}^{\kappa}\sum_{n=1}^{\kappa} A^{(\ell,m,n)}[p,q,r,s] \pm B^{(\ell,m,n)}[p,q,r,s]$$

and where $A^{(\ell,m,n)}[p,q,r,s]$ *and* $B^{(\ell,m,n)}[p,q,r,s]$ *are defined as:*

$$\begin{aligned} A^{(\ell,m,n)}[p,q,r,s] = &\frac{1}{T_s}\int_0^{T_s} p_m(t)q_{\ell-m+1}(T_s-t)r_n(t)s_{\ell-n+1}(T_s-t)dt \\ &+ \frac{1}{T_s}\int_0^{\frac{T_s}{2}} p_m(t)q_{\ell-m+1}(\frac{T_s}{2}-t)r_n(t)s_{\ell-n+1}(\frac{T_s}{2}-t)dt \\ &+ \frac{1}{T_s}\int_{\frac{T_s}{2}}^{T_s} p_m(t)q_{\ell-m+1}(\frac{3T_s}{2}-t)r_n(t)s_{\ell-n+1}(\frac{3T_s}{2}-t)dt \end{aligned}$$

and

$$\begin{aligned} B^{(\ell,m,n)}[p,q,r,s] = &\frac{1}{T_s}\int_0^{\frac{T_s}{2}} p_m(t)q_{\ell-m+1}(T_s-t)r_n(\frac{T_s}{2}-t)s_{\ell-n+1}(\frac{T_s}{2}+t)dt \\ &+ \frac{1}{T_s}\int_{\frac{T_s}{2}}^{T_s} p_m(t)q_{\ell-m+1}(T_s-t)r_n(\frac{3T_s}{2}-t)s_{\ell-n+1}(t-\frac{T_s}{2})dt \\ &+ \frac{1}{T_s}\int_0^{\frac{T_s}{2}} p_m(t)q_{\ell-m+1}(\frac{T_s}{2}-t)r_n(\frac{T_s}{2}-t)s_{\ell-n+1}(t)dt \\ &+ \frac{1}{T_s}\int_{\frac{T_s}{2}}^{T_s} p_m(t)q_{\ell-m+1}(\frac{3T_s}{2}-t)r_n(\frac{3T_s}{2}-t)s_{\ell-n+1}(t)dt. \end{aligned}$$

Proof: The proof is a direct consequence of the definition of $\eta^{\pm}(p,q,r,s)$ and the Riemann integral. Details are omitted due to the space constraints. ■

The above lemma allows us to express $\eta^{\pm}(p,q,r,s)$ as a function of integrals of the analog waveform sections $p_m(t), q_m(t), r_m(t), s_m(t)$. This turns out to be very convenient for the following result, which provides an asymptotic relationship among different $\eta^{\pm}(p,q,r,s)$ with respect to the derivatives of the corresponding pulses.

Proposition B.1. *Under the above assumptions and definitions, we can write*

$$\begin{aligned} \eta^{\pm}(p',q,r,s) - \eta^{\pm}(p,q',r,s) + \eta^{\mp}(p,q,r',s) - \eta^{\mp}(p,q,r,s') = &-\left[\mathbf{U}^{\mp}\mathcal{R}(p,q)\mathcal{R}^T(r,s)\mathbf{U}^{\pm}\right]_{1,1} \\ &-\left[\mathbf{U}^{\mp}\mathcal{R}(p,q)\mathcal{R}^T(r,s)\mathbf{U}^{\pm}\right]_{M+1,M+1} \\ &-\left[\mathbf{U}^{\pm}\mathcal{S}(p,q)\mathcal{S}^T(r,s)\mathbf{U}^{\mp}\right]_{1,1} \\ &-\left[\mathbf{U}^{\pm}\mathcal{S}(p,q)\mathcal{S}^T(r,s)\mathbf{U}^{\mp}\right]_{M+1,M+1} + O(M^{-1}) \end{aligned} \tag{20}$$

Proof: Consider the definition of $A^{(\ell,m,n)}[p,q,r,s]$ and $B^{(\ell,m,n)}[p,q,r,s]$. These terms consist of a number of integrals of a differentiable function on a compact interval of the positive real axis. Hence, we can use the

fundamental theorem of calculus to write

$$\bar{\eta}^{\pm}\left(p',q,r,s\right)-\bar{\eta}^{\pm}\left(p,q',r,s\right)+\bar{\eta}^{\mp}\left(p,q,r',s\right)-\bar{\eta}^{\mp}\left(p,q,r,s'\right)=\sum_{\ell=1}^{2\kappa-1}\phi_{\ell}$$

where

$$\begin{aligned}
\phi_{\ell} &= \mu_{\ell}\left(T_s,0\right)\xi_{\ell}\left(T_s,0\right)-\mu_{\ell}\left(0,T_s\right)\xi_{\ell}\left(0,T_s\right)\\
&\pm\left[\mu_{\ell}\left(T_s,0\right)-\mu_{\ell}\left(0,T_s\right)\right]\xi_{\ell}\left(T_s/2,T_s/2\right)\\
&\pm\mu_{\ell}\left(T_s/2,T_s/2\right)\left[\xi_{\ell}\left(0,T_s\right)-\xi_{\ell}\left(T_s,0\right)\right]\\
&+\mu_{\ell}\left(T_s/2,0\right)\xi_{\ell}\left(T_s/2,0\right)-\mu_{\ell}\left(0,T_s/2\right)\xi_{\ell}\left(0,T_s/2\right)\\
&+\mu_{\ell}\left(T_s,T_s/2\right)\xi_{\ell}\left(T_s,T_s/2\right)-\mu_{\ell}\left(T_s/2,T_s\right)\xi_{\ell}\left(T_s/2,T_s\right)\\
&\mp\mu_{\ell}\left(T_s/2,0\right)\xi_{\ell}\left(0,T_s/2\right)\pm\mu_{\ell}\left(0,T_s/2\right)\xi_{\ell}\left(T_s/2,0\right)\\
&\mp\mu_{\ell}\left(T_s,T_s/2\right)\xi_{\ell}\left(T_s/2,T_s\right)\pm\mu_{\ell}\left(T_s/2,T_s\right)\xi_{\ell}\left(T_s,T_s/2\right)
\end{aligned}$$

and where we have defined

$$\begin{aligned}
\mu_{\ell}\left(t_1,t_2\right) &= \sum_{m=1}^{\kappa}p_m(t_1)q_{\ell-m+1}(t_2)\\
\xi_{\ell}\left(t_1,t_2\right) &= \sum_{m=1}^{\kappa}r_m(t_1)s_{\ell-m+1}(t_2).
\end{aligned}$$

Now, according to Lemma 5 we can replace each term $\bar{\eta}^{\pm}\left(p,q,r,s\right)$ by the corresponding $\eta^{\pm}\left(p,q,r,s\right)$ up to an error of order $O(M^{-2})$. Therefore, it suffices to prove that the right hand side of (20) is equal to $\sum_{\ell=1}^{2\kappa-1}\phi_{\ell}+O(M^{-1})$. But this follows directly from the fact that

$$\begin{aligned}
\mu_{\ell}\left(T_s,0\right) &= \left[\mathcal{R}_2\left(p,q\right)\right]_{M,\ell}+O(M^{-1})\\
\mu_{\ell}\left(0,T_s\right) &= \left[\mathcal{R}_1\left(p,q\right)\right]_{1,\ell}+O(M^{-1})\\
\mu_{\ell}\left(T_s/2,T_s/2\right) &= \left[\mathcal{R}_1\left(p,q\right)\right]_{M,\ell}+O(M^{-1})\\
&= \left[\mathcal{R}_2\left(p,q\right)\right]_{1,\ell}+O(M^{-1})\\
\mu_{\ell}\left(0,T_s/2\right) &= \left[\mathcal{S}_2\left(p,q\right)\right]_{1,\ell}+O(M^{-1})\\
\mu_{\ell}\left(T_s/2,0\right) &= \left[\mathcal{S}_2\left(p,q\right)\right]_{M,\ell}+O(M^{-1})\\
\mu_{\ell}\left(T_s,T_s/2\right) &= \left[\mathcal{S}_1\left(p,q\right)\right]_{M,\ell}+O(M^{-1})\\
\mu_{\ell}\left(T_s/2,T_s\right) &= \left[\mathcal{S}_1\left(p,q\right)\right]_{1,\ell}+O(M^{-1})
\end{aligned}$$

and equivalently for ξ_{ℓ}, replacing p,q with r,s. This concludes the proof of the proposition. ■

The application of the above proposition may prove to be difficult due the presence of the term on the right hand side of (20), which is difficult to interpret. The following corollary establishes that under PR conditions, this term is zero.

Corollary 1. *Under the above assumptions and definitions, if (r,s) are PR-compliant and p,q are symmetric or anti-symmetric but have the opposite symmetry, we can write*

$$\eta^+(p',q,r,s)-\eta^+(p,q',r,s)+\eta^-(p,q,r',s)-\eta^-(p,q,r,s')=O(M^{-1}).$$

Proof: It follows from the PR conditions that $\mathbf{U}^-\mathcal{S}(r,s)$ is an all-zero matrix, whereas $\mathbf{U}^+\mathcal{R}(r,s)$ contains zeros everywhere except for the central column, which is filled with 1s. Proposition B.1 therefore establishes that

$$\begin{aligned}\eta^+(p',q,r,s)-\eta^+(p,q',r,s)+\eta^-(p,q,r',s)-\eta^-(p,q,r,s') &= [\mathcal{R}(p,q)]_{2M,\kappa}-[\mathcal{R}(p,q)]_{1,\kappa}\\ &\quad+[\mathcal{R}(p,q)]_{M,\kappa}-[\mathcal{R}(p,q)]_{M+1,\kappa}+O(M^{-1})\end{aligned}$$

and the result follows from symmetry. ∎

Before we conclude this appendix, we introduce another asymptotic result that will prove useful in the situation where two of the pulses meet the PR conditions.

Lemma 6. *Under the above definitions and hypotheses, assume additionally that p and q are perfect reconstruction pulses and that the analog waveforms r,s and r',s' are zero at the extreme of their support. Then, we can write*

$$\eta^\pm(p,q,r',s)-\eta^\pm(p,q,r,s')=O(M^{-2})$$

Proof: We know that $\mathbf{U}^-\mathcal{S}(p,q)$ is an all zero matrix whereas the entries of $\mathbf{U}^+\mathcal{R}(p,q)$ are all zero except for the central column, which is filled with ones. This means that $\mathrm{tr}\big[\mathbf{U}^+\mathcal{S}(p,q)\mathcal{S}(r,s)^T\big]=0$ and

$$\begin{aligned}\frac{1}{2M}\mathrm{tr}\left[\mathbf{U}^+\mathcal{R}(p,q)\mathcal{R}(r,s)^T\right] &= \frac{1}{2M}\sum_{n=1}^{2M\kappa} r[n]s[2M\kappa-n+1]\\ &= \frac{1}{T_s}\int_0^{\kappa T_s} r(t)s(\kappa T_s-t)dt+O(M^{-2})\end{aligned}$$

where the last identity follows from the Riemann integral definition. Therefore, since

$$\frac{1}{T_s}\int_0^{\kappa T_s} r'(t)s(\kappa T_s-t)dt-\frac{1}{T_s}\int_0^{\kappa T_s} r(t)s'(\kappa T_s-t)dt=r(\kappa T_s)s(0)-r(\kappa T_s)s(0)=0,$$

we obtain the result. ∎

REFERENCES

[1] B. Farhang-Boroujeny, "OFDM versus filter bank multicarrier," *IEEE Signal Process. Mag.*, vol. 28, no. 3, pp. 92–112, May 2011.

[2] M. Tanda et al., "Deliverable 2.1, Data-aided synchronization and initialization (single antenna)," ICT-211887 PHYDYAS, Tech. Rep., July 2008.

[3] X. Mestre, M. Majoral, and S. Pfletschinger, "An asymptotic approach to parallel equalization of filter bank based multicarrier signals," *IEEE Trans. Signal Process.*, vol. 61, no. 14, pp. 3592–3606, 2013.

[4] T. Ihalainen, T. H. Stitz, M. Rinne, and M. Renfors, "Channel equalization in filter bank based multicarrier modulation for wireless communications," *EURASIP Journal on Applied Signal Processing*, vol. 2007, no. 1, pp. 140–140, 2007.

[5] D. Waldhauser, L. Baltar, and J. Nossek, "MMSE subcarrier equalization for filter bank based multicarrier systems," in *IEEE 9th Workshop on Signal Processing Advances in Wireless Communications, 2008. SPAWC 2008.* IEEE, 2008, pp. 525–529.

[6] L. Baltar, D. Waldhauser, J. Nossek *et al.*, "MMSE subchannel decision feedback equalization for filter bank based multicarrier systems," in *IEEE International Symposium on Circuits and Systems, 2009. ISCAS 2009.* IEEE, 2009, pp. 2802–2805.

[7] A. Ikhlef and J. Louveaux, "An enhanced MMSE per subchannel equalizer for highly frequency selective channels for FBMC/OQAM systems," in *IEEE 10th Workshop on Signal Processing Advances in Wireless Communications, 2009. SPAWC'09.* IEEE, 2009, pp. 186–190.

[8] A. I. Prez-Neira, M. Caus, R. Zakaria, D. L. Ruyet, E. Kofidis, M. Haardt, X. Mestre, and Y. Cheng, "MIMO Signal Processing in Offset-QAM Based Filter Bank Multicarrier Systems," *IEEE Trans. Signal Process.*, vol. 64, no. 21, pp. 5733–5762, Nov 2016.

[9] T. Ihalainen, A. Ikhlef, J. Louveaux, and M. Renfors, "Channel equalization for multi-antenna FBMC/OQAM receivers," *IEEE Trans. Veh. Technol.*, vol. 60, no. 5, pp. 2070–2085, 2011.

[10] M. Caus, A. Pérez-Neira *et al.*, "Transmitter-receiver designs for highly frequency selective channels in MIMO FBMC systems," *IEEE Trans. Signal Process.*, vol. 60, no. 12, pp. 6519–6532, 2012.

[11] M. Caus, A. I. Perez-Neira, and M. Moretti, "SDMA for FBMC with block diagonalization," in *2013 IEEE 14th Workshop on Signal Processing Advances in Wireless Communications (SPAWC)*, June 2013, pp. 709–713.

[12] Y. Cheng, P. Li, and M. Haardt, "Coordinated beamforming for the multi-user MIMO downlink using FBMC/OQAM," in *Communications, Control and Signal Processing (ISCCSP), 2014 6th International Symposium on*, May 2014, pp. 465–469.

[13] Y. Cheng, L. G. Baltar, M. Haardt, and J. A. Nossek, "Precoder and equalizer design for multi-user MIMO FBMC/OQAM with highly frequency selective channels," in *2015 IEEE International Conference on Acoustics, Speech and Signal Processing (ICASSP)*, April 2015, pp. 2429–2433.

[14] O. D. Candido, S. A. Cheema, L. G. Baltar, M. Haardt, and J. A. Nossek, "Downlink Precoder and Equalizer Designs for Multi-User MIMO FBMC/OQAM," in *WSA 2016; 20th International ITG Workshop on Smart Antennas*, March 2016, pp. 1–8.

[15] X. Mestre and D. Gregoratti, "A parallel processing approach to filterbank multicarrier MIMO transmission under strong frequency selectivity," in *2014 IEEE International Conference on Acoustics, Speech and Signal Processing (ICASSP)*. IEEE, 2014, pp. 8078–8082.

[16] ——, "Parallelized Structures for MIMO FBMC Under Strong Channel Frequency Selectivity," *IEEE Trans. Signal Process.*, vol. 64, no. 5, pp. 1200–1215, March 2016.

[17] A. Paulraj, R. Nabar, and D. Gore, *Introduction to Space-Time Wireless Communications*. Cambridge university press, 2003.

[18] M. G. Bellanger, "Specification and design of a prototype filter for filter bank based multicarrier transmission," in *IEEE International Conference on Acoustics, Speech, and Signal Processing*, vol. 4. IEEE, 2001, pp. 2417–2420.